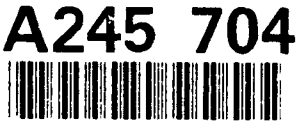

(2)

# FORMULATION OF A BULK BOUNDARY LAYER MODEL WITH PARTIAL MIXING AND CLOUDINESS

by 1990

David A. Randall

and

Qingqiu Shao



N00014-84-J-1364

Colorado State University



## DEPARTMENT OF ATMOSPHERIC SCIENCE



PAPER NO. 460



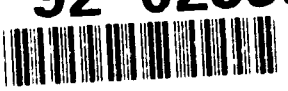

# Formulation of A Bulk Boundary Layer Model With Partial Mixing and Partial Cloudiness

David A. Randall

Qingqiu Shao

*Department of Atmospheric Science*
*Colorado State University*
*Fort Collins, Colorado 80523*

## ABSTRACT

The classical cloud-topped mixed-layer model is generalized to allow for arbitrary fractional cloudiness and incomplete mixing.

The boundary-layer depth and turbulence kinetic energy (TKE) are prognostically determined. The large turbulent eddies that contain most of the TKE and are primarily responsible for the fluxes are modeled as convective circulations, with ascending and descending branches. By assuming that the ventilation and entrainment layers at the lower and upper edges of the PBL are dominated by small-scale turbulence in quasiequilibrium, boundary conditions are developed for the rising and sinking branches of the convective circulations, and also for the scalar variances associated with the convective circulations. The convective mass flux and the fractional area covered by updrafts are diagnosed by the model. Fractional cloudiness occurs when the ascending branches are saturated and the descending branches are not.

We use a modified bulk formula in which the square root of the TKE takes the place of the wind speed. The advantages of this approach are discussed. The entrainment rate is also assumed to be proportional to the square root of the TKE; the proportionality factor depends on the inversion Richardson number, and also on an additional parameter that represents the effects of evaporative cooling when clouds are present.

The ventilation mass flux is similarly parameterized. Instead of using a conventional bulk formula in which the wind speed is multiplied by a transfer coefficient, we use a modified bulk formula in which the square root of the TKE takes the place of the wind speed. The advantages of this approach are discussed.

Large-eddy simulations are used to validate several aspects of the model's formulation.

For the special case of a well-mixed layer, the model predicts that the fractional area covered by rising motion is near 1/2, and that dissipation in the interior of the layer is weak. When the dissipation is weak and the fractional area covered by rising motion is small, the model gives the "compensating subsidence -- detrainment" relationship that has become familiar in cumulus parameterization theories. When the dissipation is strong and the fractional area covered by rising motion is near 1/2, the model gives downgradient diffusion. For the shallow cumulus regime, the model predicts that the fractional area covered by rising motion is smaller for the case of large-scale rising motion than for that of large-scale sinking motion.

A number of idealized dry cases are simulated to illustrate the model's ability to predict the development and evolution of partially mixed states. More extensive results, including both overcast and partly cloudy cases, are presented in a companion paper.

## 1. Introduction

In recent years, two new approaches have emerged for including the effects of the planetary boundary layer (PBL) in large-scale models. The first, pioneered by Deardorff (1972) and further developed by Randall (1976), Benoit (1976), and Suarez *et al.* (1983), involves coupling the large-scale model with a "bulk" PBL model in which some aspects of the vertical structure of the mean state are parameterized. Among the parameters introduced to represent the mean state are the PBL depth, which is prognostically determined, and "jumps" or discontinuities at the PBL top. The use of jumps amounts to a concession that, although the fine structure near the PBL top is important for the PBL physics, it is unresolvable by any grid that can be used in a large-scale model. Extensive results from a PBL parameterization based on a bulk model have been reported by Randall *et al.* (1985). Advantages of the bulk approach are its simplicity and computational economy. A disadvantage, up to now, is its inability to represent the internal structure of the PBL.

A second approach to PBL parameterization for large-scale models is to make use of a higher-order-closure model in which one or more turbulence variables are prognostically determined. This idea has aroused widespread interest, but has been adopted in practice only by K. Miyakoda's group at the Geophysical Fluid Dynamics Laboratory (Miyakoda and Sirutis, 1977; Miyakoda *et al.*, 1983). Advantages of this approach are its relatively high degree of physical sophistication and its ability to predict the internal structure of the PBL. Disadvantages are its requirement for high vertical resolution, and its relative complexity. Both of these lead to considerable computational expense.

The present paper reports an attempt to merge these two approaches, retaining the advantages of each, and giving rise to what we call a "second-order bulk model", or S.O.B. We have developed a bulk PBL model with a simple internal vertical structure and a simple second-order closure, designed for use as a PBL parameterization in a large-scale model. The mass-flux concept has been used to parameterize the turbulent fluxes. Fig. 1 summarizes the conceptual pedigree of the S.O.B., relative to earlier models used in boundary-layer and cumulus parameterizations.

The basic framework of the model is shown in Fig. 2. The level just above the PBL top is denoted by subscript B+, while the Earth's surface is denoted by S-. We define an infinitesimal "entrainment layer" just below the PBL top, and an infinitesimal "ventilation layer" just above the Earth's surface. The concept of an entrainment layer is motivated by the observations of Caughey *et al.* (1982) and Nicholls and Turton (1986), who described it as a thin region of weak organized vertical motions and vigorous small-scale mixing. The ventilation layer is more conventionally known as the surface layer.

The depth of the PBL (in terms of pressure) is prognostically determined, and is denoted by $\delta p_M$. The generic variable $\psi$ represents a prognostic intensive scalar such as the dry static energy, the the mixing ratio of water, or a component of the horizontal wind. Area-averaged values of $\psi$ are denoted by $\overline{\psi}$. The turbulent flux of $\psi$, denoted by $F_\psi$, is defined at the top of the surface layer, and at a level just below the PBL top. These levels are denoted by subscripts S, and B, respectively. The turbulent momentum flux is also defined levels S and B.

An entrainment mass flux, E, carries mass across the PBL top, and is closely related to the turbulent fluxes near the PBL top. Correspondingly, a ventilation mass flux, $V$, is associated with the surface fluxes; in conventional parlance, $V$ is the product of the surface air density, the surface wind speed, and a transfer coefficient. For both the entrainment and ventilation layers, the model incorporates *diagnostic balances* for mass, $\overline{\psi}$, and $\overline{\psi'^2}$. The entrainment and ventilation layers are assumed to be thin enough so that such balance conditions are appropriate. Within the ventilation

layer, the turbulent fluxes have to be carried by small eddies, since the organized vertical motions associated with the convective circulations must vanish there. The ventilation layer is assumed to be thin, in the sense that the turbulent fluxes at its top are approximately equal to those at the surface. Similarly, within the entrainment layer the organized vertical motions associated with the convective circulations become negligible, so that smaller eddies must again carry the turbulent fluxes. The entrainment layer is assumed to be thin in the sense that the turbulent fluxes at its base are approximately equal to those at the PBL top.

The vertically integrated TKE of the PBL is prognostically determined, and is denoted by $e_M$. In addition, the vertically integrated scalar variances, $\overline{(\psi')^2}_M$, are diagnostically determined. Because the model makes use of these second-order turbulence variables, it can be viewed as a highly simplified second-order closure model with very coarse vertical resolution. The coarse vertical resolution is made palatable (and feasible) by the use of an explicit, prognostic PBL depth. The fine vertical structures that typically occur near the PBL top and the Earth's surface are parametrically included in the model, by methods similar to those used in mixed-layer models. This parametric representation of the vertical structures of the entrainment and ventilation layers is an alternative to explicitly resolving these thin layers; the latter approach is followed in conventional higher-order closure models and is the primary reason that such models require high vertical resolution.

## 2. Convective Mass Flux Model

The "convective mass flux" concept introduced by Arakawa (1969) has been used by Betts (1973, 1983), Albrecht, *et al.* (1979), Hanson (1981), Penc and Albrecht (1986), Wang-and Albrecht (1986, 1990), Randall (1987), and Chatfield and Brost (1987) to construct models of PBLs containing a single family of convective circulations. The circulations have both ascending and descending branches, and many of the papers just cited considered the possibility that cloudiness can occur (or not) in either branch. None of these boundary-layer models is complete, since none has included a method to determine $\sigma$, the fractional area covered by rising motion. Although Arakawa (1969) suggested that the convective mass flux could be determined by considering the convective kinetic energy balance, the PBL models mentioned above have not addressed this issue. Most of them have also retained the "well mixed" assumption, with the notable exceptions of Betts (1973) and Albrecht *et al.* (1979). The "convective circulation" concept has also been used in observational studies (based on conditional sampling and/or joint distribution functions) by Lenschow and Stephens (1980, 1982), Greenhut and Khalsa (1982), and Wilczak and Businger (1983), Mahrt and Paumier (1984), Grossman (1984), Khalsa and Greenhut (1985), and Penc and Albrecht (1986). Recently, it has been used to analyze the results of large eddy simulations, by Schmidt and Schumann (1989).

We assume that, in the interior of the PBL, the turbulent fluxes are entirely due to the convective circulations, with rising branches covering fractional area $\sigma$, and sinking branches covering fractional area $1 - \sigma$. Observations based on conditional sampling methods suggest that $\sigma$ is typically less than 1/2 for the clear convective PBL (e.g., Lenschow and Stephens, 1980), and greater than 1/2 for the cloud-topped PBL (e.g., Nicholls, 1989).

Consider an arbitrary scalar $\psi$, satisfying a conservation equation of the form

$$\frac{\partial}{\partial t}(\rho\psi) = -\nabla\cdot(\rho V\psi) - \frac{\partial}{\partial z}(\rho w\psi) + S_\psi , \tag{2.1}$$

where $\rho$ is the density, which is quasiconstant in time and the horizontal, as in the usual anelastic approximation; $V$ is the horizontal velocity vector; $w$ is the vertical velocity; and $S_\psi$ is the source of $\psi$ per unit mass per unit time. The local time derivative and the $\nabla$ operator are defined on constant height surfaces. Putting $\psi \equiv 1$ in (2.1) gives the corresponding mass conservation equation:

$$0 = -\nabla \cdot (\rho V) - \frac{\partial}{\partial z}(\rho w). \tag{2.2}$$

Following Arakawa and Schubert (1974), we can apply (2.1) and (2.2) to an updraft of fractional area $\sigma$:

$$\frac{\partial}{\partial t}(\rho\sigma\psi_u) = -\left\{\nabla\cdot\left(\sigma\rho\overline{V\psi}\right) + \nabla\cdot\left[\sigma\rho\overline{V}\left(\psi_u - \overline{\psi}\right)\right]\right\} + \rho(\mu\psi_d - \nu\psi_u)$$
$$-\frac{\partial}{\partial z}(\rho w_u \sigma\psi_u) - \rho\tau_{dis}^{-1}\sigma\left(\psi_u - \overline{\psi}\right) + \left[-\frac{\partial}{\partial z}\left(\sigma f_{\psi,u}\right) + \sigma S_{\psi,u}\right], \tag{2.3}$$

$$\rho\frac{\partial\sigma}{\partial t} = -\nabla\cdot\left(\sigma\rho\overline{V}\right) + \rho(\mu - \nu) - \frac{\partial}{\partial z}(\rho w_u \sigma); \tag{2.4}$$

and to a downdraft of fractional area $(1 - \sigma)$:

$$\frac{\partial}{\partial t}[\rho(1-\sigma)\psi_d] = -\left\{\nabla\cdot\left[\rho(1-\sigma)\overline{V\psi}\right] + \nabla\cdot\left[\rho(1-\sigma)\overline{V}\left(\psi_d - \overline{\psi}\right)\right]\right\} - \rho(\mu\psi_d - \nu\psi_u)$$
$$-\frac{\partial}{\partial z}[\rho w_d(1-\sigma)\psi_d] - \rho\tau_{dis}^{-1}(1-\sigma)\left(\psi_d - \overline{\psi}\right)$$
$$+\left\{-\frac{\partial}{\partial z}\left[(1-\sigma)f_{\psi,d}\right] + (1-\sigma)S_{\psi,d}\right\}, \tag{2.5}$$

$$\rho\frac{\partial}{\partial t}(1-\sigma) = -\nabla\cdot\left[\rho(1-\sigma)\overline{V}\right] - \rho(\mu - \nu) - \frac{\partial}{\partial z}\left[\rho w_d(1-\sigma)\right]. \tag{2.6}$$

Note that, because $\sigma$ is variable in time, there are local time-rate-of-change terms in (2.4) and (2.6), even with the anelastic approximation. The air entering rising parcels has been assumed to have the average properties of the sinking parcels, and vice versa. Area averages satisfy

$$\left(\overline{\ }\right) = (\ \ )_u\sigma + (\ \ )_d(1-\sigma), \tag{2.7}$$

where an overbar denotes an area average (over a grid box, say); this notation will be used only where necessary to avoid confusion. Subscripts u and d denote upward and downward moving

parcels, respectively. We can interpret $\mu^{-1}$ and $\nu^{-1}$ as time scales for mass flow from downdrafts into updrafts, and from updrafts into downdrafts, respectively. The vertical turbulent flux of $\psi$ due to small eddies is denoted by $f_\psi$. The time scale for destruction of the convective circulations by lateral mixing due to smaller-scale turbulence is $\tau_{dis}$.

Arakawa and Schubert (1974) considered an arbitrary number of families of convective updrafts, called subensembles, coexisting in a single environment. Each family of updrafts was assumed to occupy a negligible fraction of the large-scale area under consideration. This "small-$\sigma$" assumption allowed them to treat the various subensembles independently, without considering direct mechanical interactions between convective elements. In effect, the updrafts were assumed to be far apart. For deep cumulus clouds, this assumption can be empirically justified, to some extent. For convective circulations in the PBL, on the other hand, there is no basis to assume that $\sigma$ is negligible compared with one; in fact, observations show the opposite (e.g., Lenschow and Stephens, 1980; 1982). If we considered multiple families of convective updrafts, it would be necessary to allow for the possibility of direct mechanical interactions among these families. A wish to avoid such complexities, and our need to consider finite $\sigma$, force us to restrict ourselves to a single family of convective circulations.

The $f_\psi$ and $\tau_{dis}$ terms of (2.4) and (2.6) represent vertical fluxes and the effects of lateral mixing, respectively. Both of these are associated with "small eddies" that appear as turbulence from the point of view of the convective circulations. As already mentioned, the small-eddy fluxes are logically necessary near the top and bottom of the PBL, where the organized vertical motions associated with the convective circulations must vanish. We shall assume later that the small-eddy fluxes are negligible in the interior of the PBL, but for the time being we carry them along for generality.

The $\tau_{dis}$ terms of (2.3) and (2.5) also require some comment. As discussed by Randall and Huffman (1982), for the case of cumulus convection, in which narrow turbulent updrafts occupy a broad, non-turbulent environment, and the turbulence has a sharp boundary at the cloud edge, the effects of such small-eddy lateral mixing are essentially included in the entrainment and detrainment terms of (2.3) and (2.5) (involving $\mu$ and $\nu$); they need not and should not be separately included as "mixing" terms. This may not be the case for PBL plumes, however, which can have significant turbulence in both their ascending and descending branches. The $\tau_{dis}$ terms of (2.3) and (2.5) are, therefore, retained to allow for the possibility of such mixing.

Adding (2.4) and (2.6), and (2.3) and (2.5), and using (2.7), we recover the area-averaged conservation equations for mass and $\overline{\psi}$ :

$$0 = -\nabla \cdot \left(\rho \overline{V}\right) - \frac{\partial}{\partial z}\left(\rho \overline{w}\right), \tag{2.8}$$

$$\frac{\partial}{\partial t}\left(\rho \overline{\psi}\right) = -\nabla \cdot \left(\rho \overline{V}\,\overline{\psi}\right) - \frac{\partial}{\partial z}\left[\rho \overline{w}\,\overline{\psi} + \left(\overline{f_\psi} + \overline{f_\psi}\right)\right] + \overline{S}_\psi. \tag{2.9}$$

Naturally, all terms involving $\mu$, $\nu$, and $\tau_{dis}$ have dropped out of (2.8-9), and $\sigma$ no longer appears explicitly. In (2.9), the turbulent fluxes associated with the convective circulations are represented by

$$\mathcal{F}_\psi = \rho\overline{w'\psi'} = \rho\left[(w_u-\overline{w})(\psi_u-\overline{\psi})\sigma+(w_d-\overline{w})(\psi_d-\overline{\psi})(1-\sigma)\right]$$
$$= M_c(\psi_u-\psi_d), \tag{2.10}$$

where

$$M_c \equiv \rho\sigma(1-\sigma)(w_u-w_d) \tag{2.11}$$

is the convective mass flux. The total turbulent flux of $\psi$ is $F_\psi = \mathcal{F}_\psi + \overline{f_\psi}$.

By vertically integrating (2.4) and (2.6) through the PBL depth, and adding the results, we obtain

$$\frac{\partial}{\partial t}\delta p_M + \nabla\cdot\left(\delta p_M \overline{V}_M\right) - gE = 0. \tag{2.12}$$

Similarly, by vertically integrating (2.3) and (2.5) through the PBL depth, adding, and using hydrostatics, we find that

$$\frac{\partial}{\partial t}\left(\delta p_M \overline{\psi_M}\right) + \nabla\cdot\left(\int_{p_{B+}}^{p_S}\overline{V\psi}\,dp\right) - gE\overline{\psi}_{B+}$$
$$= g\left(\mathcal{F}_\psi + \overline{f_\psi}\right)_S + \delta p_M \rho^{-1}\left(\overline{S}_\psi\right)_M. \tag{2.13}$$

In (2.12-13), subscript M denotes an average through the PBL depth (except in the case of $\delta p_M$). We recognize (2.12-13) as the "mixed-layer" equations, except that the horizontal advection term of (2.13) takes into account the vertical structures of $V$ and $\psi$.

Our problem now reduces to determining the turbulent flux profiles and the cloudiness. To accomplish this, we develop a method to find the updraft and downdraft properties, including $\sigma$, as well as the convective mass flux $M_c$ and the additional mass fluxes associated with entrainment and ventilation.

## 3. Boundary conditions on $\psi$ and $F_\psi$

*a)Fluxes*

The surface fluxes are assumed to satisfy the usual bulk aerodynamic formula,

$$(F_\psi)_S = V(\overline{\psi}_{S-} - \overline{\psi}_S), \tag{3.1}$$

where $V$ is the "ventilation mass flux," which is usually written as the product of surface wind speed, a transfer coefficient, and the surface air density. Our method to determine $V$ is discussed later. We now assume that the fluxes at the top of the ventilation layer are entirely due to the

convective circulations, and that the small eddy fluxes are negligible. Using this assumption with (2.10), (3.1), and also using our assumption that the ventilation layer is thin, we can write

$$V(\overline{\psi}_{S-} - \overline{\psi}_S) = M_{cS}(\psi_u - \psi_d)_S. \tag{3.2}$$

This condition implies a consistency between the fluxes obtained from the bulk formula and those determined from the mass flux model. Wang and Albrecht (1990) did not impose (3.2) or the corresponding condition at the PBL top.

At level S, the parcels rising away from the lower boundary must be "charged" with the properties of the boundary. We cannot assume, however, that the properties of the updrafts at level S are *the same* as those of the boundary, because there can be very strong gradients across the ventilation layer. The small eddies of the ventilation layer rapidly dilute air that has been in contact with the boundary, by mixing it with air that has recently descended from the interior of the PBL. As a result, $|\overline{\psi}_{S-} - \overline{\psi}_S| >> |(\psi_u - \psi_d)_S|$; from (3.2), this implies that $M_{cS} >> V$. In order to take this into account, we introduce a nondimensional parameter, $\chi_V$, such that

$$(\psi_u)_S - \overline{\psi}_S = \chi_V(\overline{\psi}_{S-} - \overline{\psi}_S); \tag{3.3}$$

in case $\chi_V = 1$, we get $(\psi_u)_S = \psi_S$. Smaller values of $\chi_V$ indicate stronger mixing by the small eddies of the ventilation layer. We expect $0 < \chi_V << 1$. By combining (2.7), (3.2), and (3.3), we find that

$$\chi_V M_{cS} = V(1 - \sigma_S). \tag{3.4}$$

This is a "continuity equation" for the eddies, expressing a relationship between the convective mass flux and the ventilation mass flux.

In the preceding discussion, it has been tacitly assumed that $\chi_V$ is independent of $\psi$, i. e., that a single "mixing" parameter $\chi_V$ satisfies (3.3) whether $\psi$ is moist static energy, total water mixing ratio, or some other intensive scalar. This assumption is supported by (3.4); if $M_{cS}$, $V$, and $\sigma_S$ are all independent of $\psi$, then $\chi_V$ must also be independent of $\psi$. Such independence suggests that $\chi_V$ is a useful concept.

We now apply a similar analysis to the entrainment layer. The assumption that the entrainment layer is thin yields the familiar "jump" relation between $(F_\psi)_B$ and the entrainment rate:

$$(F_\psi)_B = -E(\overline{\psi}_{B+} - \overline{\psi}_B) - \int_{z_B}^{z_{B+}} \overline{S_\psi}\, dz. \tag{3.5}$$

Here we follow Lilly (1968) by keeping the $S_\psi$ term, which represents a possible concentrated entrainment-layer "source" of $\psi$, (e.g., due to radiation). We assume now that the fluxes at the base of the entrainment layer are entirely due to the convective circulations, and that the "small-eddy" fluxes are negligible. Then, by comparing (2.10) and (3.5), and using (2.7), we obtain

$$M_{cB}(\psi_d - \overline{\psi})_B = E\sigma_B(\overline{\psi}_{B+} - \overline{\psi}_B) + \sigma_B \int_{z_B}^{z_{B+}} \overline{S_\psi}\, dz. \tag{3.6}$$

At this point, we introduce a mixing parameter $\chi_E$, by analogy with (3.3). To allow for the effects of the concentrated source, however, we include an additional term:

$$(\psi_d - \overline{\psi})_B = \chi_E(\overline{\psi}_{B+} - \overline{\psi}_B) + \lambda \int_{z_B}^{z_{B+}} \overline{S_\psi}\, dz. \tag{3.7}$$

Here $\lambda$ is a coefficient that will be determined later. According to (3.7), the properties of the descending air at level B are related to those of the free atmosphere just above the PBL top, as modified by small-eddy mixing and the effects of any concentrated source within the entrainment zone. Since there is a sharp gradient of $\psi$ across the entrainment layer, we expect $0 < \chi_E << 1$.

The mixing parameter $\chi_E$ is closely related to the parameter $\chi$ discussed by Siems *et al.* [1989; see also Albrecht *et al.* (1985) and Nicholls and Turton (1986)]. We can interpret $\chi_E$ as the value of $\chi$ associated with the downdraft air at level B. Further discussion is given later in this Section, and also in Appendix C.

Comparing (3.6) with (3.7), we find that

$$(-M_{cB}\chi_E + E\sigma_B)(\overline{\psi}_{B+} - \overline{\psi}_B) + (-M_{cB}\lambda + \sigma_B)\int_{z_B}^{z_{B+}} \overline{S_\psi}\, dz = 0. \tag{3.8}$$

In case the source term of (3.8) vanishes, we obtain

$$\chi_E M_{cB} = E\sigma_B. \tag{3.9}$$

This relationship does not involve $\psi$; it must, therefore, apply for *all* $\psi$. To ensure that (3.9) will be satisfied even when the source term of (3.8) is not zero, we must choose

$$\lambda = \sigma_B / M_{cB}. \tag{3.10}$$

We can interpret (3.9) as another "continuity equation", analogous to (3.4). Again, we have tacitly assumed that $\chi_E$ is independent of the species under consideration. This assumption is consistent with (3.9), since $M_{cB}$, $E$, and $\sigma_B$ are independent of species. We can use (3.9) to eliminate $M_{cB}$ in (3.6), or, alternatively, use (3.10) to eliminate $\lambda$ in (3.7); either way, the result is:

$$\psi_{dB} = \chi_E \overline{\psi_{B+}} + (1 - \chi_E)\overline{\psi}_B + \frac{\chi_E}{E} \int_{z_B}^{z_{B+}} \overline{S_\psi}\, dz. \tag{3.11}$$

According to (3.11), the descending air at level B has the properties of the free atmosphere, except as modified by mixing (when $\chi_E < 1$) and by the concentrated source. Caughey *et al.* (1982) and Nicholls (1989) have reported observations of cool downdrafts in the upper portions of stratocumulus cloud sheets. They concluded that the sinking air had been radiatively cooled near the cloud top. Such effects are represented by the $S_\psi$ term of (3.11).

Since this term is inversely proportional to E, we conclude that radiative cooling in the entrainment layer can produce negatively buoyant parcels most effectively if the entrainment rate is small. This suggests that entrainment driven by radiative cooling near cloud-top tends to be self-limiting.

According to (3.4), ventilation-layer dilution becomes more effective (in other words, $\chi_V$ decreases) as the convective mass flux increases relative to $V(1 - \sigma_S)$. The ventilation mass flux times the fractional area covered by the incoming downdrafts is a measure of the rate at which the updrafts leaving the ventilation layer can be supplied with air that has been charged with surface properties, and the convective mass flux is a measure of the rate at which this air is removed from the surface layer. The stronger the convective mass flux becomes, the less effectively ventilation-layer air can be charged with surface properties before it is carried away into the interior of the PBL. A similar interpretation can be given for (3.9).

*b) Updrafts and downdrafts: The cloud-free case*

The next step is to introduce a further simple relation between $\chi$ and $\sigma$, variations of which can be applied to both the ventilation and entrainment layers. First consider the ventilation layer. Within the ventilation layer there exist parcels with many different virtual dry static energies, essentially spanning the range between $\overline{s_{vS-}}$ and $\overline{s_{vS}}$. (A few parcels can have virtual dry static energies which lie outside this range, but we neglect their influence for simplicity.) The various parcels are produced by mixing, in various proportions, air from the interior of the PBL with air that has been charged with surface properties. For the ventilation layer, we define $\chi$ without a subscript as follows: For each ventilation-layer parcel, $\chi$ is the mixing fraction of the air with surface properties, so that, under dry adiabatic mixing (for which the virtual dry static energy is approximately conserved), we have

$$s_v(\chi) = \chi\overline{s_{vS-}} + (1-\chi)\overline{s_{vS}}. \tag{3.12}$$

This definition allows us to specify the properties of a parcel by giving the value of $\chi$ associated with it.

*We now assume that the parcels emerging from the ventilation layer into the rising branches of the convective circulations have properties representative of the lightest (warmest in the sense of virtual dry static energy) parcels available in the ventilation layer.* (Note that this assumption *does not* restrict us to unstable cases in which the rising parcels are positively buoyant.)

Let the probability density function (pdf) for $\chi$ in the ventilation layer be denoted by $\Pi_v(\chi)$. Then $\Pi_v(\chi)d\chi$ gives the probability of encountering, in the ventilation layer, a parcel whose properties correspond to a value of $\chi$ in the range $(\chi, \chi + d\chi)$. According to our assumption, the average virtual dry static energy of the updraft air emerging from the ventilation layer is then given by

$$\left(s_{v_u}\right)_S = \frac{\int_{\text{warmest parcels}} s_v(\chi)\Pi_v(\chi)d\chi}{\int_{\text{warmest parcels}} \Pi_v(\chi)d\chi}.$$

(3.13)

We now assume that

$$\sigma_S = \int_{\text{warmest parcels}} \Pi_v(\chi)d\chi\ .$$

(3.14)

Recall that $\sigma_S$ is, by definition, the fractional area covered by updrafts at level S. On the other hand, $\int_{\text{warmest parcels}} \Pi_v(\chi)d\chi$ is the cumulative fraction of all ventilation-layer parcels that must be mixed together to create a mixture with the properties of the updrafts at level S, assuming that this mixture is to be generated by choosing first the very lightest parcels, then the second lightest, and so on. According to our assumption (3.14), these two fractions are equal. To see why this should be so, imagine that we have the power to physically rearrange the ventilation layer air into any spatial configuration that we choose. We could then vertically "stack" the air to be incorporated into updrafts, inside the ventilation layer. The fractional area covered would then be $\int_{\text{warmest parcels}} \Pi_v(\chi)d\chi$, and this would obviously be equal to $\sigma_S$.

It follows, of course, that the fractional area covered by downdrafts at level S, namely $1 - \sigma_S$, must be equal to the remaining fraction of all parcels in the ventilation layer, namely $1 - \int_{\text{warmest parcels}} \Pi_v(\chi)d\chi$. It *does not* follow, however, that the convective downdrafts at level S are composed of the densest parcels available in the ventilation layer. This would be true only if the average properties of all parcels in the ventilation layer were the same as the area-averaged properties of the air at level S.

By using (3.14) in (3.13), we obtain

$$\left(s_{v_u}\right)_S \sigma_S = \int_{\text{warmest parcels}} s_v(\chi)\Pi_v(\chi)d\chi.$$

(3.15)

Now use (3.3) with $\psi \equiv s_v$ on the left-hand side of (3.15), and (3.12) on the right-hand side. This leads immediately to

$$\sigma_S \chi_V = \int_{\text{warmest parcels}} \chi\Pi_v(\chi)d\chi.$$

(3.16)

Finally, use (3.4) to eliminate $\chi_V$ in (3.16). This leads to

$$V\sigma_S(1-\sigma_S) = M_{cS} \int_{\text{warmest parcels}} \chi \Pi_V(\chi) d\chi .$$

(3.17)

Consider a simple example, motivated by the following idea. Parcels with properties very close to those of the surface itself make up only a tiny fraction of all the parcels available in the ventilation layer, so that $\Pi_V(\chi)$ is very small for values of $\chi$ near one, and increases significantly only as $\chi$ decreases to values near zero. Consider a "step-function" pdf; suppose that $\Pi_V(\chi)$ is zero for $\chi_A \le \chi \le 1$, and assumes a constant value $\hat{\Pi}_V$ for $0 \le \chi \le \chi_A$ (see Fig. 3). Since

$$\int_0^1 \Pi_V(\chi) d\chi = 1,$$

(3.18)

we have

$$\chi_A \hat{\Pi}_V = 1.$$

(3.19)

Note that the case of constant $\Pi_V(\chi)$ is included here; it corresponds to $\hat{\Pi}_V = 1$. Of course, $\hat{\Pi}_V$ cannot be less than one.

Consider first the unstable case, for which $\overline{s_{vS-}}$ is greater than $\overline{s_{vS}}$. Then the lightest parcels available are those for which $\chi = \chi_A$, and progressively denser parcels are encountered as $\chi$ decreases towards zero. Let $\chi_{\min}$ be the value of $\chi$ characteristic of the *densest* parcels that are incorporated into the convective updrafts. With these assumptions, and using (3.19), we find that (3.14) and (3.17) reduce to

$$\chi_{\min} = \frac{1-\sigma_S}{\hat{\Pi}_V},$$

(3.20)

and

$$V\sigma_S(1-\sigma_S) = M_{cS}\hat{\Pi}_V \int_{\chi_{\min}}^{\chi_A} \chi \, d\chi .$$

(3.21)

respectively. Integrating (3.21), and using (3.19) and (3.20) to eliminate $\chi_A$ and $\chi_{min}$, respectively, we obtain

$$\sigma_S = \frac{\hat{\Pi}_V \dfrac{V}{M_{cS}} - 1}{\hat{\Pi}_V \dfrac{V}{M_{cS}} - \frac{1}{2}}.$$

(3.22)

This is a useful result. It tells how to obtain $\sigma_S$ for given values of $\hat{\Pi}_V V$ and $M_{cS}$.

The stable case differs, because the lightest parcels are those which consist mainly of air from the interior of the PBL, i.e. those with $\chi$ near zero. If we continue to use the model represented by Fig. 3, we find in place of (3.22) that

$$\sigma_S = \frac{\hat{\Pi}_V \frac{V}{M_{cS}}}{\hat{\Pi}_V \frac{V}{M_{cS}} + \frac{1}{2}}. \tag{3.23}$$

To have $\chi_v \equiv 0$, we need $\sigma_S \cong 0$ or sufficiently large $\hat{\Pi}_V$.

We now apply a similar analysis to the entrainment layer. *We assume that the descending parcels in the convective circulations at level B are formed from the densest parcels available in the entrainment layer.* (This assumption *does not* restrict us to unstable cases in which the sinking parcels are negatively buoyant.) The various parcels are produced by mixing, in various proportions, air from the interior of the PBL with air that has recently been entrained. For the entrainment layer, define $\chi$ without a subscript as follows: for each entrainment-layer parcel, $\chi$ is the mixing fraction of the air with free-atmospheric properties. Under dry adiabatic mixing, we have

$$s_v(\chi) = \chi \overline{s_{vB+}} + (1-\chi)\overline{s_{vB}}. \tag{3.24}$$

In such dry adiabatic cases, the entrainment-layer parcels with the lowest virtual dry static energies are those for which $\chi$ is zero. [Cloudy cases with phase changes and radiative cooling are discussed at the end of this Section.]

Let the pdf for $\chi$ in the entrainment layer be denoted by $\Pi_E(\chi)$. When (3.24) is satisfied, the average virtual dry static energy of the sinking air emerging from the entrainment layer is

$$\left(s_{vd}\right)_B = \frac{\int_{\text{coldest parcels}} s_v(\chi)\Pi_E(\chi)d\chi}{\int_{\text{coldest parcels}} \Pi_E(\chi)d\chi}. \tag{3.25}$$

By analogy with (3.14), we assume that

$$1-\sigma_B = \int_{\text{coldest parcels}} \Pi_E(\chi)d\chi\,. \tag{3.26}$$

Use of (3.26) in (3.25) gives

$$(s_{vd})_B(1-\sigma_B) = \int_{\text{coldest parcels}} s_v(\chi)\Pi_E(\chi)d\chi . \tag{3.27}$$

Now use (3.11) with $\psi \equiv s_v$ and $\overline{S_\psi} = 0$ on the left-hand side of (3.27), and (3.24) on the right-hand side. This gives

$$(1-\sigma_B)\chi_E = \int_{\text{coldest parcels}} \chi\Pi_E(\chi)d\chi . \tag{3.28}$$

Finally ,we use (3.9) to eliminate in (3.28). The result is

$$E\sigma_B(1-\sigma_B) = M_{cB} \int_{\text{coldest parcels}} \chi\Pi_E(\chi)d\chi . \tag{3.29}$$

Parcels with properties very close to those of the free atmosphere itself make up only a tiny fraction of all the parcels available in the entrainment layer at any given time, so that $\Pi_E(\chi)$ is very small for values of $\chi$ near one, and increases significantly only as $\chi$ decreases to values near zero. Suppose that $\Pi_E(\chi)$ is zero for $\chi_B \le \chi \le 1$, and assumes a constant value $\hat{\Pi}_E$ for $0 \le \chi \le \chi_B$. (In principle this is the same "step-function" pdf that we discussed for the ventilation layer and sketched in Fig. 3, except that the width of the step is not necessarily the same; hence, we use the notation $\chi_B$ in discussing the entrainment layer, in place of $\chi_A$ for the ventilation layer.) Clearly, we must have

$$\chi_B\hat{\Pi}_E = 1. \tag{3.30}$$

The case of constant $\Pi_E(\chi)$ is included here; it corresponds to $\hat{\Pi}_E = 1$. Of course, $\hat{\Pi}_E$ cannot be less than one.

The PBL is normally capped by an inversion, so that the densest parcels available are those for which $\chi$ is near zero. A straightforward analysis leads to

$$\sigma_B = \frac{1}{2\hat{\Pi}_E\dfrac{E}{M_{cB}} + 1}. \tag{3.31}$$

If the mean virtual dry static energy should happen to decrease upward across the entrainment layer, the densest parcels available will have $\chi \equiv \chi_B$. For such a statically unstable entrainment layer, we find that

$$\sigma_B = \frac{1}{2\hat{\Pi}_E \frac{E}{M_{cB}} - 1}.$$

(3.32)

Now we combine our results for the ventilation and entrainment layers. First, consider the clear convective PBL (unstable ventilation layer) capped by an inversion (stable entrainment layer), and suppose that $\sigma$ and $M_c$ are independent of height. This allows us to drop the subscripts S and B from these two variables. By combining (3.22) and (3.31), we obtain

$$M_c = 2\left[-\hat{\Pi}_E E + \sqrt{\left(\hat{\Pi}_E E\right)^2 + \hat{\Pi}_E E \hat{\Pi}_V V}\right].$$

(3.32)

This expression always gives $M_c \geq 0$. It follows from (3.31) that $0 \leq \sigma \leq 1$.

There are, in addition, three other possible combinations of stable and unstable entrainment and ventilation layers. Table 1 gives the forms of $M_c$ and $\sigma$ for all four possibilities. In each case, it turns out that $M_c$ and $\sigma$ depend only on two parameters, namely $\hat{\Pi}_V V$ and $\hat{\Pi}_E E$. In fact, $\sigma$ depends only on the ratio of these two parameters, $\eta \equiv \frac{\Pi_E E}{\Pi_V V}$. The normalized mass flux, $\frac{M_c}{\sqrt{\Pi_E E \Pi_V V}}$, also depends only on $\eta$.

Fig. 4 shows how the normalized mass flux and $\sigma$ vary with $\eta$, for each case. Without exception, $M_c \geq 0$ and $0 \leq \sigma \leq 1$. From this point of view, the model is quite well behaved. Note that in all four cases $\sigma$ decreases as $\eta$ increases. This means that *strong entrainment is associated with small* $\sigma$. When the ventilation layer is unstable and the entrainment layer is stable, the normalized mass flux decreases as $\eta$ increases. The reverse is true when the ventilation layer is stable and the entrainment layer is unstable. When both layers are unstable, the normalized mass flux is maximized when $\eta = 1$. When both layers are stable, the normalized mass flux is independent of $\eta$.

*b) Updrafts and downdrafts: Extension to the cloudy case*

In writing (3.12) and (3.24), we have assumed that the virtual dry static energy is conserved under dry adiabatic mixing, in both the entrainment and ventilation layers. This assumption is not valid for the cloud-capped PBL.

First, consider a case for which only moist and/or dry adiabatic processes occur in the entrainment layer, so that radiative cooling is not an issue. Then we can simply make use of thermodynamic variables that are conserved under both moist adiabatic and dry adiabatic mixing, e.g. the moist static energy, $h$, and the total mixing ratio, $r$. Mixtures satisfy

$$h(\chi) = \chi \overline{h_{B+}} + (1-\chi)\overline{h_B},$$

(3.33)

$$r(\chi) = \chi \overline{r_{B+}} + (1-\chi)\overline{r_B}. \tag{3.34}$$

The virtual dry static energy of a mixture at level B can be obtained from

$$s_v(\chi) = s_v\left[h(\chi), r(\chi), p_B\right], \tag{3.35}$$

using straightforward thermodynamic methods (see Appendix C). Then, if $\Pi_E(\chi)$ is known, we can proceed in essentially the same way as before. In particular, (3.26) and (3.29) apply without modification. When $s_v$ increases monotonically with $\chi$, (3.31) holds as before. It is hard to imagine a cloudy case in which $s_v$ decreases monotonically with $\chi$, but if such a thing were to happen, we could apply (3.32).

An interesting complication arises when a parcel formed by mixing a cloudy parcel and a clear parcel can be denser, for some values of $\chi$, than either of the two parcels from which it is derived (Squires, 1958; Lilly, 1968; Randall, 1980; Deardorff, 1980; Albrecht *et al.*, 1985; Nicholls and Turton, 1986; Siems *et al.*, 1989). This opens up the possibility of cloud-top entrainment instability (CTEI). When conditions are right for CTEI, the densest possible mixtures consist of parcels containing a finite fraction of free-atmospheric air. The limits of integration in (3.26) and (3.29) must then be adjusted so as to include the densest available parcels.

Fig. 5 illustrates an example of this situation. The numerical values used to construct this example are given in the figure caption. These have been chosen so that CTEI is predicted by the criterion of Randall (1980), with $\Delta s_v - (\Delta s_v)_{crit}$ = - 2000 kJ kg$^{-1}$, but not by the criterion of Siems *et al.* (1989), with $D$ = 0.3 (see Appendix E for a definition of $D$). The curve in Fig. 5 shows $s_v(\chi) - \overline{s_{vB}}$, plotted as a function of $\chi$. By methods discussed in Appendix C, we can identify the densest possible mixture and the associated value of $\chi$. Following the notation of Siems *et al.* (1989), we let $\chi_*$ denote the value of $\chi$ for which the virtual dry static energy is minimized. In this case, $\chi_*$ = 0.05, i.e. the coldest parcels are almost entirely composed of air with in-cloud properties. This is in line with earlier analyses (e.g., Albrecht *et al.*, 1985). We choose first these densest parcels, then the second densest, and continue in this way until some fraction of the available parcels have been chosen, spanning values of $\chi$ from $\chi_{min}$ to $\chi_{max}$, such that $s_v(\chi_{min}) = s_v(\chi_{max})$. As illustrated in Fig. 5, the population of selected parcels will usually be asymmetric in $\chi$-space; more will be chosen on the low-$\chi$ side, and fewer on the high-$\chi$ side. Using an assumed form of $\Pi_E(\chi)$, and for the range of selected parcels, we evaluate the integrals in (3.26) and (3.29). These effectively determine $\sigma_B$ and $E / M_{cB}$. In this way, for a given form of $\Pi_E(\chi)$, we can plot $\sigma_B$ as a function of $E / M_{cB}$, essentially determining a relation analogous to those given by (3.31-32). Details are discussed in Appendix C.

The results for the example of Fig. 5 are shown in Fig. 6, with the step-function distribution of $\Pi_E(\chi)$, and $\hat{\Pi}_E = 1$. Also shown in Fig. 6 are the corresponding curves predicted by (3.31) and (3.32). Since $s_v(\chi)$ is almost monotonically increasing with $\chi$, it is not surprising that this cloudy example nearly agrees with the predictions of (3.31) for stable inversion case.

Figs. 7 and 8 give a second example, chosen to be subject to CTEI by *both* the criteria of Randall (1980), with $\Delta s_v - (\Delta s_v)_{crit}$ = - 5000 kJ kg$^{-1}$, *and* the criterion of Siems *et al.* (1989), with $D$ = 1.5. The numerical values used are given in the caption for Fig. 7. The liquid water mixing ratio corresponding to the conditions at level B is 3.2 g kg$^{-1}$, much larger than would be encountered in coastal stratocumulus clouds. Fig. 7 shows $s_v(\chi) - \overline{s_{vB}}$ as a function of $\chi$. The virtually coldest parcels available are those for which $\chi$ = 0.30, i.e. such parcels contain a substantial fraction of free-atmospheric air. The implied relationship between $\sigma_B$ and $E / M_{cB}$, is shown in Fig. 8, again for $\hat{\Pi}_E = 1$. As before, the predictions of (3.31) and (3.32) are also shown in the figure. This unstable cloudy case departs significantly from (3.31), and is intermediate between (3.31) and (3.32).

When radiative cooling occurs in the entrainment layer, (3.33) must be modified to take into account the radiatively induced moist static energy decrease that each parcel experiences, as a function of $\chi$. We can write

$$h(\chi) = \chi \overline{h_{B+}} + (1-\chi)\overline{h_B} + \delta h_R(\chi), \tag{3.36}$$

where $\delta h_R(\chi)$ represents the effects of radiation on the parcel's moist static energy. Obviously, there must be some relationship between $\overline{\Delta R}$ and an integral of $\delta h_R(\chi)$; this will be explained below. Fig. 9 schematically illustrates three profiles of $h(\chi)$, for different choices of $\delta h_R(\chi)$ . Of course, when $\delta h_R(\chi)$ is zero, $h(\chi)$ varies linearly with $\chi$. This is the dotted curve in the figure. The dashed curve illustrates the situation for which $\delta h_R(\chi)$ is negative and independent of $\chi$, so that $h(\chi)$ is simply shifted uniformly to smaller values. The third curve in Fig. 9 illustrates a case in which $\delta h_R(\chi)$ is more strongly negative for smaller values of $\chi$. This may be realistic; more cooling will accrue to parcels that spend more time inside the cloud, but near the cloud edge; and less to parcels that spend more time outside the cloud. Such parcels should have small values of $\chi$, i.e. properties characteristic of the cloud layer rather than the inversion. The effect is that cooler parcels are cooled more.

As mentioned above, an integral of $\delta h_R(\chi)$ must correspond to the correct area-averaged radiative cooling. This constraint can be imposed as follows. By analogy with (3.24), we can write

$$(h_d)_B = \frac{\int_{\text{coldest parcels}} h(\chi)\Pi_E(\chi)\,d\chi}{\int_{\text{coldest parcels}} \Pi_E(\chi)\,d\chi}. \tag{3.37}$$

Here the limits of integration are understood to be chosen so as to encompass the coldest parcels available. Substituting from (3.26) and (3.36), we obtain

$$(h_d)_B = \frac{\int_{\text{coldest parcels}} \left[\chi \overline{h_{B+}} + (1-\chi)\overline{h_B} + \delta h_R(\chi)\right] \Pi_E(\chi) d\chi}{1-\sigma_B}. \tag{3.38}$$

A second expression for $(h_d)_B$ can be obtained from (3.11), with $h \equiv \psi$:

$$h_{dB} = \chi_E \overline{h_{B+}} + (1-\chi_E)\overline{h_B} - \frac{\chi_E}{E}\overline{\Delta R}. \tag{3.39}$$

In (3.39), we have replaced the "source integral" of (3.11) by $-\overline{\Delta R}$. We now require that the radiation terms of (3.38) and (3.39) agree. With the use of (3.9), this implies that

$$\sigma_B(1-\sigma_B)\overline{\Delta R} = -M_{c,B} \int_{\text{coldest parcels}} \delta h_R(\chi) \Pi_E(\chi) d\chi, \tag{3.40}$$

which is the desired constraint on $\delta h_R(\chi)$. If $\delta h_R(\chi)$ is independent of $\chi$ for the range of $\chi$ in question, (3.40) reduces to

$$\sigma_B \overline{\Delta R} = -M_{c,B} \delta h_R . \tag{3.41}$$

For a given distribution of $\delta h_R(\chi)$, we can work out $s_v(\chi)$, essentially from (3.36) and (3.35). We then identify the densest available parcels, in the usual way.

*d) Summary*

In this Section, we have analyzed the entrainment and ventilation layers, and their coupling with the interior of the PBL. By requiring consistency among the various fluxes, and applying "boundary conditions" on the updraft properties at the top of the ventilation layer and the downdraft properties at the base of the entrainment layer, we obtained (3.4) and (3.9), which express relationships among mass fluxes, fractional areas, and mixing parameters.

We then assumed that the parcels entering updrafts at the top of the ventilation layer are the lightest ones available, and that those entering downdrafts at the base of the entrainment layer are the densest ones available. Using these assumptions, we are able to derive relationships among the fractional areas and the mass fluxes, when the pdfs for virtual dry static energy in the entrainment and ventilation layers are known. For the case of "step function" pdfs, these are given by (3.22-23) and (3.31-32).

Next, for the case in which $\sigma$ and $M_c$ are independent of height, we obtained expressions for $\sigma$ and $M_c$, given in Table 1. These can be used to determine $\sigma$ and $M_c$ in a numerical model.

Finally, we showed how these results can be generalized for the cloudy PBL.

Further discussion of the boundary conditions on the scalar variances is given in Appendix D.

At present, we use the idealized "step function" probability density functions discussed in this Section. The constant values assigned are $\hat{\Pi}_V = 10$ and $\hat{\Pi}_E = 10$.

## 4. Prediction equations for $\sigma$ and the scalar variances

The "plume" equations derived in Section 2 determine how $\sigma$ and the scalar variances associated with the plumes vary in time.

To derive an expression for $\partial\sigma / \partial t$, subtract (2.6) from (2.4) to obtain

$$2\rho\frac{\partial\sigma}{\partial t} + \nabla\cdot\left[(2\sigma - 1)\rho\overline{V}\right] - 2\rho(\mu - \nu) + \frac{\partial}{\partial z}\left\{\rho\left[w_u\sigma - w_d(1-\sigma)\right]\right\} = 0. \tag{4.1}$$

Using (2.8) and the identity

$$\rho\left[w_u\sigma - w_d(1-\sigma)\right] = 2M_c - \rho\overline{w}(1-2\sigma),$$

which can be derived from (2.7) and (2.11), we can rewrite (4.1) as

$$\rho\frac{\partial\sigma}{\partial t} + \rho\overline{V}\cdot\nabla\sigma + \rho\overline{w}\frac{\partial\sigma}{\partial z} = -\frac{\partial M_c}{\partial z} + \rho(\mu - \nu). \tag{4.2a}$$

Using (2.8) again, this can be recast in "flux" form:

$$\rho\frac{\partial\sigma}{\partial t} + \nabla\cdot\left(\rho\overline{V}\sigma\right) + \frac{\partial}{\partial z}\left(\rho\overline{w}\sigma\right) = -\frac{\partial M_c}{\partial z} + \rho(\mu - \nu). \tag{4.2b}$$

When the terms on the left-hand-sides of (4.2a - b) are negligible, we obtain

$$0 = -\frac{\partial M_c}{\partial z} + \rho(\mu - \nu), \tag{4.2c}$$

which was derived by Arakawa and Schubert (1974).

We now introduce the conservation equation for the variance of $\psi$ that is associated with the convective circulations. As shown in Appendix B, this is

$$\left(\frac{\partial}{\partial t}+\overline{V}\cdot\nabla+\overline{w}\frac{\partial}{\partial z}\right)\left[\sigma(1-\sigma)(\psi_u-\psi_d)^2\right]+\frac{1}{\rho}\frac{\partial}{\partial z}\left[M_c(1-2\sigma)(\psi_u-\psi_d)^2\right]$$
$$=-\frac{2\mathcal{F}_\psi}{\rho}\frac{\partial\overline{\psi}}{\partial z}-\left[(\mu+\nu)+2\tau_{dis}^{-1}\sigma(1-\sigma)\right](\psi_u-\psi_d)^2+2(\psi_u-\psi_d)Z_\psi,$$

(4.3)

where

$$Z_\psi=\rho^{-1}\left\{-(1-\sigma)\frac{\partial}{\partial z}(f_{\psi,u}\sigma)+\sigma\frac{\partial}{\partial z}\left[f_{\psi,d}(1-\sigma)\right]+\sigma(1-\sigma)\left(S_{\psi,u}-S_{\psi,d}\right)\right\}.$$

(4.4)

We retain, in (4.4),the terms representing small-eddy fluxes, even though, as already mentioned, we assume that these are negligible except in the ventilation and entrainment layers.

Using conventional Reynolds averaging, we find corresponding to (4.3) that

$$\left(\frac{\partial}{\partial t}+\overline{V}\cdot\nabla+\overline{w}\frac{\partial}{\partial z}\right)\left(\overline{\psi'^2}\right)+\frac{1}{\rho}\frac{\partial}{\partial z}\left(\rho\overline{w'\psi'^2}\right)$$
$$=-\nabla\cdot\left(\overline{V'\psi'^2}\right)+2\left[-\overline{V'\psi'}\cdot\nabla\overline{\psi}-\frac{F_\psi}{\rho}\frac{\partial\overline{\psi}}{\partial z}-\varepsilon_\psi+\overline{\psi'S'}_\psi\right].$$

(4.5)

Here $\varepsilon_\psi$ is the molecular dissipation rate, per unit mass. Comparison of (4.3) with (4.5) reveals a term-by-term correspondence. In particular,

$$\rho\overline{w'\psi'^2}=M_{cc}(\psi_u-\psi_d)^2,$$

(4.6)

where

$$M_{cc}=(1-2\sigma)\sigma(1-\sigma)\rho(w_u-w_d)$$

(4.7)

is a mass flux which plays the same role for transport of the second moments as $M_C$ plays for transport of the first moments. The expression for $M_{CC}$ given in (4.7) emerges naturally in the course of the derivation given in Appendix B. It can also be derived by a method analogous to that used in (2.10). Note that the sign of $M_{CC}$ is determined by the value of $\sigma$. Variance is transported upward for $\sigma < 1/2$, and downward for $\sigma > 1/2$. This fact is of some importance, and will be discussed further later.

The damping factor $\sigma(1-\sigma)\tau_{dis}^{-1}$, which appears in (4.3), can be simplified by noting that small eddies will be most effective at reducing the differences between the ascending and descending branches of the plumes when one of the two branches is much narrower than the other, and least effective when the two branches have the same width. On this basis, we assume that $T_{dis}^{-1}\equiv\sigma(1-\sigma)\tau_{dis}^{-1}$ is independent of $\sigma$. Then we obtain

$$\left(\frac{\partial}{\partial t}+\overline{V}\cdot\nabla+\overline{w}\frac{\partial}{\partial z}\right)\left[\sigma(1-\sigma)(\psi_u-\psi_d)^2\right]+\frac{1}{\rho}\frac{\partial}{\partial z}\left[M_c(1-2\sigma)(\psi_u-\psi_d)^2\right]$$
$$=-\frac{2\mathcal{F}_\psi}{\rho}\frac{\partial\overline{\psi}}{\partial z}-\left[(\mu+\nu)+2T_{dis}^{-1}\right](\psi_u-\psi_d)^2+2(\psi_u-\psi_d)Z_\psi . \tag{4.8}$$

It is also possible to work out a prognostic equation for $\overline{\psi'^3}$, following a derivation very similar to that for $\overline{\psi'^2}$, as given in Appendix B. We can show, however, that

$$\frac{\overline{\psi'^3}}{\left(\overline{\psi'^2}\right)^{3/2}}=\frac{(1-2\sigma)}{\sqrt{\sigma(1-\sigma)}}, \tag{4.9}$$

which implies that prediction of $\overline{\psi'^3}$ contributes essentially the same information as prediction of $\sigma$ itself. The triple moment equations are, therefore, redundant. Similarly, any higher moments of $\psi$ can be related to $\overline{\psi'^2}$ by simple functions of $\sigma$. In this sense, the familiar turbulence closure problem posed by an infinite succession of independent moments does not occur in the present model. The reason is that $\psi$ can take only two values, namely $\psi_u$ and $\psi_d$.

## 5. Balance equations for the scalar variances

We now explore some implications of the results of the preceding Section, by considering simplified special cases. Neglecting the local time-change and large-scale advection terms of (4.8), we find that

$$\frac{\partial}{\partial z}\left[M_c(1-2\sigma)(\psi_u-\psi_d)^2\right]$$
$$=-2\mathcal{F}_\psi\frac{\partial\overline{\psi}}{\partial z}-\rho\left[(\mu+\nu)+2T_{dis}^{-1}\right](\psi_u-\psi_d)^2+2\rho(\psi_u-\psi_d)Z_\psi , \tag{5.1}$$

i.e., transport balances the combined effects of dissipation and production. We can further simplify (5.1) by using (4.2c) to obtain:

$$\mathcal{F}_\psi\mathcal{D}+(1-2\sigma)\frac{\partial\mathcal{F}_\psi}{\partial z}=-M_c\frac{\partial\overline{\psi}}{\partial z}+\rho Z_\psi , \tag{5.2}$$

where

$$\mathcal{D}\equiv-\frac{\partial\sigma}{\partial z}+\rho M_c^{-1}\left[\mu\sigma+\nu(1-\sigma)+T_{dis}^{-1}\right]. \tag{5.3}$$

We can interpret $\mathfrak{D}$, which has the units of inverse length, as a measure of the importance of dissipative processes. The $\partial\sigma/\partial z$ term of (5.3) arises from the transport term of (5.1). The quantity in square brackets is never negative, so $\mathfrak{D} \geq 0$ unless $\sigma$ increases strongly upward. Since observations (e.g., Lenschow and Stephens, 1980) suggest that $\sigma$ typically *decreases* upward, we expect $\mathfrak{D} > 0$.

Several conclusions can be drawn from (5.2-3), by considering the case $Z_\psi = 0$.

First, if $(1 - 2\sigma) / \mathfrak{D}$ is small ($\sigma$ near 1/2 and strong dissipation), we get

$$\mathfrak{f}_\psi \equiv -\frac{M_c}{\mathfrak{D}} \frac{\partial \overline{\psi}}{\partial z}. \tag{5.4}$$

This is a downgradient diffusion formula, with diffusion coefficient $M_c / \mathfrak{D}$.

Next, consider a layer that is well-mixed in several conservative variables $\psi_1$, $\psi_2$, etc, so that (5.2) reduces to

$$\mathfrak{D}\mathfrak{f}_\psi + (1-2\sigma)\frac{\partial \mathfrak{f}_\psi}{\partial z} = 0. \tag{5.5}$$

The fluxes are determined in part by the free-atmospheric values of the various $\psi$'s, so we cannot satisfy (5.5) for all $\psi$ by imposing constraints on the fluxes. The *only* way to satisfy (5.5) simultaneously for *all* of the variables is to put

$$\mathfrak{D} = 0, \tag{5.6}$$

$$\sigma = 1/2. \tag{5.7}$$

Since, according to (5.7), $\sigma$ is a constant, (5.3) implies that $\mathfrak{D}$ is the sum of two non-negative terms. Then (5.6) implies that each term must be zero, so that

$$M_c = \text{constant}, \tag{5.8}$$

$$T_{dis}^{-1} = 0. \tag{5.9}$$

Referring back to (5.1), we find a trivial balance in which gradient production, transport, and dissipation all vanish. (Recall that the variance transport by triple correlations is zero when $\sigma = 1/2$.) Deardorff (1974, his Fig. 13) obtained such a balance for the virtual dry static energy variance budget in the interior of a numerically simulated convective well mixed layer for which (5.7) was approximately satisfied.

Deardorff(1966) discussed the countergradient heat flux often observed in the convective PBL, i.e. the potential temperature flux is often observed to be upward even though the mean

potential temperature increases upwared. Deardorff considered a balance between gradient production on the one hand (which is negative in the case of a countergradient potential temperature flux) and the transport of potential temperature variance by the convection. For the present model, this means $\mathcal{D} = 0$, so that (5.2) reduces to

$$(1-2\sigma)\frac{\partial \mathcal{F}_\theta}{\partial z} = -M_c \frac{\partial \overline{\theta}}{\partial z}. \tag{5.10}$$

In a convective PBL, the potential temperature is being increased by the convection, so that $\partial \mathcal{F}_\theta / \partial z < 0$. Observations show that in such situations $\sigma = 1/2$ (e.g. Lenschow and Stephens, 1980). Then, since the convective mass flux is positive, (5.10) implies that the potential temperature increases upward, in agreement with the observations.

Finally, suppose that $\mathcal{D}$ is small (weak dissipation). Then (5.2) reduces to

$$(1-2\sigma)\frac{\partial \mathcal{F}_\psi}{\partial z} \cong -M_c \frac{\partial \overline{\psi}}{\partial z}. \tag{5.11}$$

This balance is characteristic of the temperature and moisture budgets of tropical cumulus layers, in which $\sigma$ is small and "compensating subsidence" produces the convective effects on the mean profiles. Arakawa (1969) derived (5.11), for the case of small $\sigma$; it has also been discussed by Ooyama (1971) and Arakawa and Schubert (1974), among others. [The "detrainment" term discussed by Arakawa and Schubert (1974) is also present in (5.2-3); it arises from the gradient of $M_c$ in (5.3), for the case of outflow in which $\mu = 0$ and $\nu > 0$.]

In fact, $\mathcal{D}$ actually should be small for the case of deep convection. First of all, $\sigma$ is small at every level, so $\partial\sigma/\partial z$ is small. For the case of entrainment ($\mu > 0$ and $\nu = 0$), the middle term of (5.3) reduces to $\sigma$ times the "fractional entrainment rate" discussed in cumulus parameterization theories (e.g., Arakawa and Schubert, 1974), so it will also be small because $\sigma$ is small. Finally, the $T_{dis}$ term of (5.3) represents the dissipation due to small-eddy mixing, which is confined to the interiors of the convective clouds. For the case of deep convection, these clouds cover only a tiny fraction of the large-scale area (again, $\sigma$ is small), so that this term cannot be very large. Evidently each term contributing to $\mathcal{D}$ is individually small for the case of deep convection.

For the cumulus regime, the conservation equation for $\overline{\psi}$ in the entrainment layer can be approximated by a balance between vertical advection and convective transport, i.e.

$$\frac{\partial \mathcal{F}_\psi}{\partial z} \cong -\rho \overline{w} \frac{\partial \overline{\psi}}{\partial z}. \tag{5.12}$$

Comparing (5.11) and (5.12), we find that

$$\sigma = \tfrac{1}{2}\left(1 - \frac{M_c}{\rho \bar{w}}\right). \tag{5.13}$$

For tropical cumulus layers with large-scale rising motion, it is observed that $M_c \approx \rho \bar{w}$, so that (5.13) is consistent with observations that show $\sigma << 1$. Alternatively, we can conclude from (5.13) that if $\sigma << 1$, we must have $M_c \approx \rho \bar{w}$. For the case of large-scale sinking motion, (5.13) predicts larger values of $\sigma$, again in qualitative agreement with observations.

The preceding discussion shows that (5.2-3) are consistent with a variety of observed balances in convective layers. In effect, they provide a physically based interpolation between the "compensating subsidence" and "mixing length" regimes.

We now investigate simple analytic solutions of (5.2) for $Z\psi = 0$. For this purpose, we rewrite (5.2) as

$$\mathcal{D}\mathcal{F}_\psi + s\frac{\partial \mathcal{F}_\psi}{\partial z} = -M_c \frac{\partial \bar{\psi}}{\partial z}, \tag{5.14}$$

where, for convenience, we have defined

$$s \equiv 1 - 2\sigma. \tag{5.15}$$

We regard (5.14) as a first-order linear ordinary differential equation for $\mathcal{F}_\psi$, in which the $M_c$ term represents a forcing. If $\mathcal{D}$, $s$, and the forcing are assigned particular vertical profiles (e.g., linear or quadratic in z), then (5.14) can be solved by elementary analytical methods.

Two preliminary comments are in order. First, the solution of (5.14) must be well behaved when $s = 0$. This compels us to discard the homogeneous solution; only the particular solution is physically relevant. Second, inspection of (5.14) shows that $\mathcal{D}\delta z_M$ must be less than or comparable to one; larger values would imply ludicrous vertical profiles of $\bar{\psi}$. Recall from (5.3) that consists of contributions due to the vertical variations of $\sigma$ and $M_C$, as well as those due to small-eddy dissipation, as represented by the $T_{dis}$ term. For values of $\mathcal{D}\delta z_M$ on the order of one, the implied dissipation times $T_{dis}$ turn out to be extremely long by PBL standards -- on the order of many hours. This strongly suggests that, to the extent that $\mathcal{D}\delta z_M$ is different from zero, it is associated with vertical variations of $\sigma$ and/or $M_C$, but not with small-eddy dissipation. From this point on, we assume $T_{dis} \to \infty$. We also assume that $M_C$ is constant with height.

Suppose that

$$\sigma = \sigma_0 + \sigma_1 \zeta ,$$

(5.16)

where $\sigma_0$ and $\sigma_1$ are constants, and

$$\zeta \equiv \frac{z}{\delta z_M};$$

(5.17)

and let

$$M_c \frac{\partial \overline{\psi}}{\partial \zeta} = a_\psi + b_\psi \zeta ,$$

(5.18)

where $a_\psi$ and $b_\psi$ are constants. With these assumptions, the particular solution of (5.13) turns out to be of the form

$$\psi = (\psi)_S + \zeta \left[ (\psi)_B - (\psi)_S \right],$$

(5.19)

and consistency requires

$$a_\psi = \sigma_1 (\psi)_S - (1 - 2\sigma_0) \left[ (\psi)_B - (\psi)_S \right],$$

(5.19)

$$b_\psi = 3\sigma_1 \left[ (\psi)_B - (\psi)_S \right].$$

(5.20)

Substituting (5.20-21) back into (5.187), we find that

$$\frac{\partial \overline{\psi}}{\partial \zeta} = M_c^{-1} \left\{ (\psi)_S \left[ (1 - 2\sigma_0) + \sigma_1 (1 - 3\zeta) \right] + (\psi)_B \left[ -(1 - 2\sigma_0) + 3\sigma_1 \zeta \right] \right\}.$$

(5.21)

This is similar in form to Eq.(46) of Wyngaard and Brost (1984).

Suppose for simplicity that $\overline{\psi}$ is simply linear with height. Then from (5.21) it follows that $\sigma_1$ must be zero; in other words, $\sigma$ must be uniform with height. For this case, (5.21) reduces to

$$\frac{\partial \overline{\psi}}{\partial \zeta} = \frac{-1}{M_c} \left\{ (1 - 2\sigma) \left[ (\psi)_B - (\psi)_S \right] \right\}.$$

(5.22)

From (5.22), we can evaluate $\overline{\psi_S}$ and $\overline{\psi_B}$:

$$\overline{\psi_S} = \overline{\psi_M} + \left\{ \frac{(1-2\sigma)}{2M_c} \left[ \left( \mathcal{F}_\psi \right)_B - \left( \mathcal{F}_\psi \right)_S \right] \right\}, \tag{5.23}$$

$$\overline{\psi_B} = \overline{\psi_M} - \left\{ \frac{(1-2\sigma)}{2M_c} \left[ \left( \mathcal{F}_\psi \right)_B - \left( \mathcal{F}_\psi \right)_S \right] \right\}. \tag{5.24}$$

We can also use (5.22) to interpret some of the departures from "well mixedness" that have been observed in nature. For example, suppose that $\left( \mathcal{F}_\psi \right)_S >> \left( \mathcal{F}_\psi \right)_B$ and $\sigma < 1/2$. This could be the case of dry static energy in a typical clear convective PBL capped by an inversion. Then (5.22) reduces to

$$\frac{\partial \overline{\psi}}{\partial \zeta} = \frac{(1-2\sigma)\left( \mathcal{F}_\psi \right)_S}{M_c}. \tag{5.25}$$

According to observations (e.g. Deardorff, 1966), $\overline{\psi}$ should increase upward, as predicted by (5.25).

As a second example, suppose that $\left( \mathcal{F}_\psi \right)_B$ is more strongly upward than $\left( \mathcal{F}_\psi \right)_S$. This can happen in the case of the moisture flux, with rapid entrainment of very dry upper-level air. For such a case, (5.22) predicts that $\overline{\psi}$ decreases upward. An upward decrease of the mean water vapor mixing ratio is often observed.

Finally, note that for $\sigma = 1/2$, (5.22) predicts that all conservative variables are well mixed. This is consistent with our earlier analysis.

These results encourage us to believe that (5.22) can account for the observed variability of $\frac{\partial \overline{\psi}}{\partial \zeta}$.

## 6. Ventilation and entrainment mass fluxes

We relate the ventilation mass flux to the TKE by

$$V = \rho_S c_e \sqrt{e_M}, \tag{6.1}$$

where $c_e$ is a transfer coefficient that must be parameterized. In (6.1), the square root of the TKE is playing the role more conventionally played by the mean wind speed. One way of rationalizing (6.1) is that *turbulent fluxes cannot occur unless TKE exists.* The existence of a mean wind favors the production of TKE, although it is not logically necessary for the existence of TKE. Since $\sqrt{e_M}$

is typically an order of magnitude smaller than the mean wind speed, $c_e$ is typically an order of magnitude larger than the conventional transfer coefficient; a nominal value of $c_e$ is 0.02.

It appears that (6.1) has at least two major advantages over the usual bulk aerodynamic formula. First, it behaves well in the limiting case of free convection, for which the mean wind speed vanishes even though the TKE and the surface energy fluxes can be vigorous. Second, $c_e$ should be relatively well behaved near neutral stability, where the transfer coefficient used in the conventional bulk formula changes almost discontinuously from small values in the stable regime to large values in the unstable regime. We expect that, in contrast, $c_e$ increases relatively gradually as the PBL passes from the stable to the unstable regime, simply because $e_M$ itself will increase rapidly. For purposes of this paper, no elaborate parameterization of $c_e$ is attempted; such a parameterization could be developed through the use of a large-eddy model, which would allow $e_M$ to be determined readily. That project is left to the future. For now, we simply use $c_e = 0.02$.

Our entrainment closure is based on the ideas of Breidenthal and Baker (1985). It is explained in Appendix E.

## 7. Outline of an algorithm to solve the model

Although the derivation of the model has been somewhat lengthy, its implementation is fairly simple, at least for the cloud-free case. When there are no clouds in the PBL, we can proceed as follows:

1. Initialize all prognostic variables.

2. A "first guess" for $\overline{\psi_S}$ and $\overline{\psi_B}$ can be based on the assumption that the PBL is well mixed, i.e. that $\overline{\psi_B} = \overline{\psi_S} = \overline{\psi_M}$. From $\overline{\psi_B}$, obtain $\overline{\Delta\psi}$.

3. Determine $V$ and $E$, using the parameterizations discussed in Section 6 and Appendix E, respectively. In general, this will require use of the values of $\overline{\psi_S}$ and $\overline{\psi_B}$ used above, because of the dependence of $V$ (through $c_e$) on the near-surface stability, and the dependence of $E$ on the "jumps."

4. Use $V$ and $E$ with $\overline{\psi_S}$ and $\overline{\psi_B}$ to determine $\left(\mathcal{F}_\psi\right)_S$ and $\left(\mathcal{F}_\psi\right)_B$.

5. Find $\sigma$ and $M_C$, using the methods of Section 3, with the values of $V$ and $E$ obtained above.

6. From (5.23-4), obtain revised values of $\overline{\psi_S}$ and $\overline{\psi_B}$.

7. Iterate Steps 3 - 6 to obtain a simultaneous solution for $\overline{\psi_S}$ and $\overline{\psi_B}$, $V$, $E$, $\sigma$, $M_C$, $\left(\mathcal{F}_\psi\right)_S$ and $\left(\mathcal{F}_\psi\right)_B$.

8. Having completed the iteration, it is possible to evaluate the vertical profiles of the mean fields, the turbulent fluxes, and the updraft and downdraft properties.

9. Using the results of Steps 7 and 8, work out the various terms of the prognostic equations.

10. Predict new values of the prognostic variables.

11. Return to Step 2.

When clouds are present, solution of the model becomes considerably more complicated. To see why, first recall that the radiative cooling rate affects the moist static energy flux profile. The radiation calculation cannot be done until we know what the cloudiness is. The cloudiness cannot be evaluated until we reach Step 8 of the algorithm outlined above. The added complexity of the cloudy case arises, then, because the turbulent fluxes are needed within the iteration loop that *precedes* Step 8. This means that we need a nested iteration for the cloudy case.

## 9. Summary and concluding discussion

We have presented what amounts to very simple second-order-closure model that makes use of an explicit (but highly idealized) description of a turbulent eddy: the "convective circulation." In adopting this approach, we have necessarily abandoned any pretense that the second-order closure is so general that it can apply to any type of turbulent boundary layer. On the other hand, we have benefitted by being able to use mechanistic ideas about the dynamics of individual turbulent elements, which would be difficult or impossible to express in the purely statistical framework of a conventional second-order-closure model.

"New" elements of the S.O.B. include the use of a prognostic TKE, together with an explicit PBL depth and parameterized ventilation and entrainment layers; the introduction of explicit boundary conditions on the updraft-downdraft variables, which led to our expressions for $\sigma$ and $M_C$ ; the formulation of the conservation equations for the scalar variances in terms of an explicit model of a convective circulation; and the revision of the bulk aerodynamic formula to use the square root of the TKE in place of the mean wind speed.

The model provides a way to determine $\sigma$ and $M_C$ , as well as the vertical profile of $\overline{\psi}$ inside the PBL. It encompasses the "mixing length","compensating subsidence", and "well mixed" regimes within a single physically based framework. It can represent clear, partly cloudy, and overcast boundary layers. It is simple enough to be used as a parameterization within a large-scale model.

Obviously there are many avenues for further exploration. Alternative forms of $\Pi_v(\chi)$ and $\Pi_E(\chi)$ can be investigated. Vertical variations of $\sigma$ and $M_C$ can be allowed. It may be possible to extend the model by allowing multiple layers (or in some other way allowing multiple degrees of freedom in the vertical) within the PBL. In such a multi-layer model, it may be advantageous to determine the scalar variances prognostically.

In the immediate future, we plan to test the model and explore its ramifications using both FIRE data and LES results from the model of Moeng (1984, 1986). We also plan to exercise the model in a prognostic mode.

## ACKNOWLEDGEMENTS

D. Randall has been working on this for longer than he cares to admit. Portions of this work were carried out first while he was visiting first the International Meteorological Institute of the University of Stockholm, and later the European Centre for Medium Range Weather Forecasts. Both institutions provided fine working environments.

Helpful comments were offered by Prof. Akio Arakawa, Dr. Stephen Krueger, and Dr. Howard Hanson.

Support for this research was provided by NASA's Climate Program under Grant NAG-1-893, and by the Office of Naval Research under Contract N00014-89-J-1364. Computing resources were provided by the Numerical Aerodynamic Simulation Facility at NASA/Ames.

APPENDIX A

# A Method to Predict the Vertically Integrated Turbulence Kinetic Energy

As discussed in Section 7, the vertically integrated conservation law for the TKE can be written as

$$g^{-1}\delta p_M \frac{\partial e_M}{\partial t} + E e_M = B + S - D. \tag{A.1}$$

Here $B$, $S$, and $D$ represent production by buoyancy, production by shear, and dissipation, respectively.

The vertically integrated dissipation rate and the vertically averaged TKE are assumed to be related by

$$D = \rho_M (e_M / a_1)^{3/2}, \tag{A.2}$$

where $\rho_M$ is the vertically averaged PBL density, and $a_1 \equiv 0.163$ is a dimensionless constant.

The buoyancy production integral, $B$, is of the form

$$B = \kappa \int_{p_{s+}}^{p_{s-}} \frac{F_{sv}}{p}\, dp, \tag{A.3}$$

where $\kappa$ is Poisson's constant. For the cloud-free test cases described in this paper, we have simply evaluated (A.3) using the trapezoidal rule, with data points at levels S, I, and B. A more complex approach is needed when clouds are present, and will be described in Part II.

The shear production integral, $S$, is of the form

$$S = \int_{p_{s+}}^{p_{s-}} \mathbf{F}_V \cdot \frac{\partial \overline{V}}{\partial p}\, dp. \tag{A.4}$$

We divide this integral into three parts: shear production in the surface layer, in the interior of the PBL, and in the entrainment layer. The surface layer shear production is approximately given by

$$\int_{p_s}^{p_{s-}} \mathbf{F}_V \cdot \frac{\partial \overline{V}}{\partial p}\, dp = (\mathbf{F}_V)_S \cdot \overline{V}_S = \left|(\mathbf{F}_V)_S\right| \cdot \left|\overline{V}_S\right|. \tag{A.5}$$

Here the second equality follows from the assumption that the surface stress in parallel to the surface wind.

The interior shear production is given by

$$\int_{p_B}^{p_S} \boldsymbol{F}_V \cdot \frac{\partial \overline{\boldsymbol{V}}}{\partial p}\, dp = (\boldsymbol{F}_V)_I \cdot \left[ \frac{\overline{\boldsymbol{V}_\mu} - \overline{\boldsymbol{V}_{\mu-1}}}{\delta p_M (\zeta_\mu - \zeta_{\mu-1})} \right]. \tag{A.6}$$

Finally, the entrainment layer shear production is approximately given by

$$\int_{p_{B+}}^{p_B} \boldsymbol{F}_V \cdot \frac{\partial \overline{\boldsymbol{V}}}{\partial p}\, dp = \tfrac{1}{2} \left| (\boldsymbol{F}_V)_B \right| \cdot \left| \Delta \overline{\boldsymbol{V}} \right| = \tfrac{1}{2} E \left| \Delta \overline{\boldsymbol{V}} \right|^2. \tag{A.7}$$

In (A.6), the factor of 1/2 arises because $\boldsymbol{F_V}$ decreases from $(\boldsymbol{F_V})_B$ to zero across the entrainment layer, so that its average value is $(\boldsymbol{F_V})_B$ / 2. The second equality comes from applying (3.5) to the momentum budget of the entrainment layer.

APPENDIX B

# Derivation of the Scalar Variance Conservation Equation

The convective variance of $\psi$ is

$$\begin{aligned}\overline{\psi_2'} &= \sigma\left(\psi_u - \overline{\psi}\right)^2 + (1-\sigma)\left(\psi_d - \overline{\psi}\right)^2 \\ &= \sigma(1-\sigma)\left(\psi_u - \psi_d\right)^2.\end{aligned} \tag{B.1}$$

Therefore,

$$\frac{\partial}{\partial t}\left(\overline{\psi''^2}\right) = 2\sigma(1-\sigma)\left(\psi_u - \psi_d\right)\frac{\partial}{\partial t}\left(\psi_u - \psi_d\right) + \left(\psi_u - \psi_d\right)^2(1-2\sigma)\frac{\partial \sigma}{\partial t}. \tag{B.2}$$

To obtain an expression for the first term on the right-hand-side of (B.2), we use (2.3) and (2.5) to rewrite (2.2) and (2.4) in advective form. From the resulting equations we can show that

$$\begin{aligned}&\sigma(1-\sigma)\left[\frac{\partial}{\partial t}\left(\psi_u - \psi_d\right) + \overline{V}\cdot\nabla\left(\psi_u - \psi_d\right) + w_u\frac{\partial \psi_u}{\partial z} - w_d\frac{\partial \psi_d}{\partial z}\right] + \left[\mu(1-\sigma) + \nu\sigma\right]\left(\psi_u - \psi_d\right) \\ &= -\tau_{dis}^{-1}\sigma(1-\sigma)\left(\psi_u - \psi_d\right) + \rho^{-1}\left\{-(1-\sigma)\frac{\partial}{\partial z}\left(f_{\psi,u}\sigma\right) + \sigma\frac{\partial}{\partial z}\left[f_{\psi,d}(1-\sigma)\right] + \sigma(1-\sigma)\left(S_{\psi,u} - S_{\psi,d}\right)\right\}.\end{aligned} \tag{B.3}$$

Use of

$$\begin{aligned}w_u\frac{\partial \psi_u}{\partial z} - w_d\frac{\partial \psi_d}{\partial z} &= \overline{w}\frac{\partial}{\partial z}\left(\psi_u - \psi_d\right) \\ &+ \left(w_u - w_d\right)\left[\frac{\partial \overline{\psi}}{\partial z} - \left(\psi_u - \psi_d\right)\frac{\partial \sigma}{\partial z} + (1-2\sigma)\frac{\partial}{\partial z}\left(\psi_u - \psi_d\right)\right]\end{aligned} \tag{B.4}$$

and (4.2a) in (B.3) gives

$$\sigma(1-\sigma)\left(\frac{\partial}{\partial t}+\bar{V}\cdot\nabla+\bar{w}\frac{\partial}{\partial z}\right)(\psi_u-\psi_d)+[\mu(1-\sigma)+\upsilon\sigma](\psi_u-\psi_d)$$
$$+\frac{M_c}{\rho}\left[-(\psi_u-\psi_d)\frac{\partial\sigma}{\partial z}+(1-2\sigma)\frac{\partial}{\partial z}(\psi_u-\psi_d)\right]$$
$$=-\frac{M_c}{\rho}\frac{\partial\overline{\psi}}{\partial z}-\tau_{dis}^{-1}\sigma(1-\sigma)(\psi_u-\psi_d)$$
$$+\rho^{-1}\left\{-(1-\sigma)\frac{\partial}{\partial z}\left(f_{\psi,u}\sigma\right)+\sigma\frac{\partial}{\partial z}\left[f_{\psi,d}(1-\sigma)\right]+\sigma(1-\sigma)\left(S_{\psi,u}-S_{\psi,d}\right)\right\}. \tag{B.5}$$

Now multiply (B.5) by 2 $(\psi_u - \psi_d)$, multiply (2.13) by $(\psi_u - \psi_d)^2(1-2\sigma)$, and add the results. After combining terms, and using (2.10), we obtain (4.1), which is the desired result.

APPENDIX C

# Buoyancy of Mixed Parcels

As discussed by Albrecht *et al.* (1985), Nicholls and Turton (1986), and Siems *et al.* (1989), under some conditions the density of a parcel formed by mixing clear air with cloudy air can be greater than the density of either of the contributing species. Suppose that we mix air from level B, which is assumed here to lie inside a cloud, with air from level B+,which is assumed to lie above the cloud top. The moist static energy, h, and total mixing ratio, r, of the mixture will satisfy

$$h(\chi) = \overline{h_{B+}}\chi + \overline{h_B}(1-\chi), \tag{C.1}$$

$$r(\chi) = \overline{r_{B+}}\chi + \overline{r_B}(1-\chi). \tag{C.2}$$

As $\chi$ is varied, the properties of the mixture will vary according to

$$\frac{\partial h(\chi)}{\partial \chi} = \overline{h_{B+}} - \overline{h_{B+}} \equiv \Delta \bar{h}, \tag{C.3}$$

$$\frac{\partial r(\chi)}{\partial \chi} = \overline{r_{B+}} - \overline{r_{B+}} \equiv \Delta \bar{r}. \tag{C.4}$$

As indicated in Fig. 5, the changes of the virtual dry static energy of a mixed parcel follow two nearly straight, intersecting lines as $\chi$ is varied. The line on the left side of the figure represents the set of saturated states, while that on the right side represents unsaturated states. The lines intersect where the virtual dry static energy is minimized, at $\chi = \chi_*$. Using moist thermodynamics, we can show that

$$\left[\frac{\partial s_v(\chi)}{\partial \chi}\right]_{saturated} = \Delta s_v - (\Delta s_v)_{crit}, \tag{C.5}$$

$$\left[\frac{\partial s_v(\chi)}{\partial \chi}\right]_{unsaturated} = \Delta \bar{h} - (1-\delta\epsilon) L \Delta \bar{r}, \tag{C.6}$$

where $\delta$ and $\epsilon$ are positive thermodynamic coefficients, and $(\Delta s_v)_{crit}$ is a critical inversion strength, such that when $\Delta s_v < (\Delta s_v)_{crit}$ it is possible for mixed parcels composed of air from the inversion and the cloud layer to be cooler than the cloud layer air. Further discussion is given by Randall (1980), who showed that

$$(\Delta s_v)_{crit} = \left[\frac{1-(1+\delta)\varepsilon}{1+\gamma}\right] L\left(q^*_{B+} - q_{B+}\right), \tag{C.7}$$

where $\gamma$ is another positive thermodynamic coefficient, $q^*$ is the saturation mixing ratio, and $q$ is the actual vapor mixing ratio. According to (C.7), $(\Delta s_v)_{crit}$ is a measure of the relative humidity in the inversion. Dry inversion air favors large values of $(\Delta s_v)_{crit}$.

From Fig. 5, it is apparent that the intersection of the two line segments is given by

$$s_{vB} + \chi_* \left[\frac{\partial s_v(\chi)}{\partial \chi}\right]_{saturated} = s_{vB+} + (1-\chi_*)\left[\frac{\partial s_v(\chi)}{\partial \chi}\right]_{unsaturated}. \tag{C.8}$$

Solving for $\chi_*$, and again using moist thermodynamics, we can show that

$$\chi_* = \frac{[1-(1+\delta)\varepsilon]L\ell_B}{[1-(1+\delta)\varepsilon]L\ell_B + (\Delta s_v)_{crit}}. \tag{C.9}$$

The form of (C.9) guarantees that $0 \le \chi_* \le 1$. When $\ell_B$ is zero, we have $\chi_* = 0$, and as $\ell_B$ increases $\chi_*$ approaches one. We can use (C.9) to evaluate $\chi_*$ analytically.

By substituting (C.9) back into (C.8), we can show that the minimum possible value of $s_v$ is

$$(s_v)_{\min} = s_{vB} + \left[\Delta s_v - (\Delta s_v)_{crit}\right]\left\{\frac{[1-(1+\delta)\varepsilon]L\ell_B}{[1-(1+\delta)\varepsilon]L\ell_B + (\Delta s_v)_{crit}}\right\}. \tag{C.10}$$

From (C.10) we find that the parameter $D$ defined by Siems *et al.* (1989) can be written as

$$D \equiv -\left[\frac{(s_v)_{\min} - s_{vB}}{\Delta s_v}\right] = \left\{\frac{\dfrac{(\Delta s_v)_{crit}}{\Delta s_v} - 1}{1 + \dfrac{(\Delta s_v)_{crit}}{[1-(1+\delta)\varepsilon]L\ell_B}}\right\}. \tag{C.11}$$

This result shows that $D$ is positive when $\Delta s_v - (\Delta s_v)_{crit}$ is negative, and gives a simple way of evaluating $D$ analytically.

Finally, we need a way to deal with the integrals in (3.26) and (3.29). The range of integration for the integrals is the "coldest parcels" available for a given choice of $\sigma_B$. How do we

identify the appropriate range of $\chi$ ? Fig. C1 shows *two values of* $\chi$ for which the virtual dry static energies of the mixed parcels are *the same*. The value of $\chi$ corresponding to a saturated state is called $\chi_1$, and that corresponding to an unsaturated state is called $\chi_2$. The parcels with values of between $\chi_1$ and $\chi_2$ are the coldest available for some choice of $\sigma_B$. According to (3.26), we have

$$1-\sigma_B = \int_{\text{coldest parcels}} \Pi_E(\chi)\,d\chi\ . \tag{C.12}$$

If $\Pi_E(\chi)$ takes the constant value $\hat{\Pi}_E$ for the range of $\chi$ in question, then we can write

$$1-\sigma_B = \hat{\Pi}_E(\chi_2-\chi_1). \tag{C.13}$$

A second equation involving $\chi_1$ and $\chi_2$ can be obtained by inspection of Fig. C1:

$$s_{vB}+\left[\Delta s_v-(\Delta s_v)_{crit}\right]\chi_1 = s_{vB+}-\left[\Delta h-(1-\delta\epsilon)L\Delta r\right](1-\chi_2). \tag{C.14}$$

By solving (C.13) and (C.14) simultaneously, we can determine $\chi_1$ and $\chi_2$ for a given value of $\sigma_B$. It is then straightforward to evaluate the integral in (3.29).

APPENDIX D

# Boundary Conditions on the Scalar Variances

Because $\overline{\psi}$ varies rapidly across the top of the ventilation layer and the base of the entrainment layer, there is vigorous variance production in these regions, but there is also rapid variance dissipation by small eddies. The variance budget for the ventilation layer can be expressed as

$$2\int_{z_{S-}}^{z_S} \varepsilon_\psi \rho \, dz = 2(F_\psi)_S(\overline{\psi}_{S-} - \overline{\psi_S}) - (\rho\overline{w'\psi'\psi'})_S. \tag{D.1}$$

The left-hand side of (D.1) represents dissipation. The first term on the right-hand side represents gradient production, and the second represents transport into the ventilation layer by triple correlations.

Similarly, the variance budget for the entrainment layer can be expressed as

$$2\int_{z_B}^{z_{B+}} \varepsilon_\psi \rho \, dz = -(F_\psi)_B \Delta\overline{\psi} + (\rho\overline{w'\psi'\psi'})_B - E(\overline{\psi'^2})_B + 2\int_{z_B}^{z_{B+}} \overline{\psi' S'_\psi} \, dz. \tag{D.2}$$

The left-hand side and the first two terms on the right-hand side of (D.2) are closely analogous to those of (D.1). In the gradient production term of (D.2), the minus sign appears because of the definition of $\Delta\psi$. The factor of two that appears in the production term of (D.1) is not present in the corresponding term of (D.2), because the turbulent flux of $\psi$ drops from $(F_\psi)_B$ to zero across the entrainment layer, so that its average value for the entrainment layer is *half* of $(F_\psi)_B$. The second term of (D.2) represents the transport of variance into the entrainment layer by triple correlations. The fourth term represents the rate at which scalar variance is provided to the newly entrained air. The fifth term represents variance production due to fluctuations of $S_\psi$ in the entrainment layer. There is a close analogy between (D.2) and (3.5).

Now define nondimensional measures of the dissipation rates, denoted by $k_V$ and $k_E$, respectively:

$$2\int_{z_{S-}}^{z_S} \varepsilon_\psi \rho \, dz \equiv k_V V \sigma_S(1-\sigma_S)(\psi_u - \psi_d)_S^2, \tag{D.3}$$

$$2\int_{z_B}^{z_{B+}} \varepsilon_\psi \rho \, dz \equiv k_E E \sigma_B(1-\sigma_B)(\psi_u - \psi_d)_B^2. \tag{D.4}$$

These definitions are motivated by the idea that the rates of variance dissipation in the ventilation and entrainment layers should be related to the actual values of the variances at the edges of those layers. For the ventilation layer, the results of Section 3 imply that

$$(\rho\overline{w'\psi'\psi'})_S = M_{cS}(1-2\sigma_S)(\psi_u - \psi_d)_S^2, \tag{D.5}$$

$$(F_\psi)_S = M_{cS}(\psi_u - \psi_d)_S,$$

(D.6)

$$\overline{\psi}_{S-} - \overline{\psi}_S = \chi_V^{-1}(1-\sigma_S)(\psi_u - \psi_d)_S .$$

(D.7)

Using (D.3) , (D.5-7), and (3.4) in (D.1), we can show that

$$\sigma_S = \frac{2-\chi_V}{k_V\chi_V^2 + 2(1-\chi_V)} \approx \frac{1}{1+\frac{1}{2}k_V\chi_V^2},$$

(D.8a)

or, alteratively,

$$k_V = \frac{2(1-\sigma_S)-\chi_V(1-2\sigma_S)}{\sigma_S\chi_V^2} \approx \frac{2(1-\sigma_S)}{\sigma_S\chi_V^2}.$$

(D.8b)

All reference to $\psi$ has dropped out, indicating that $k_V$ is independent of species. From (D.8b) it is apparent that $k_V$ is of order $\chi_V^{-2}$, i.e., $k_V >> 1$. This close relationship between $\chi_V$ and $k_V$ is reasonable, since stronger dissipation (larger $k_V$) and stronger mixing (smaller $\chi_V$) must both be due to more efficient small-scale eddies.

Similarly, for the entrainment layer, we have

$$(\rho\overline{w'\psi'\psi'})_B = M_{cB}(1-2\sigma_B)(\psi_u - \psi_d)_B^2,$$

(D.9)

$$(F_\psi)_B = M_{cB}(\psi_u - \psi_d)_B,$$

(D.10)

$$\Delta\psi = \chi_E^{-1}\sigma_B\left[-(\psi_u - \psi_d)_B - M_{cB}^{-1}\int_{z_B}^{z_{B+}} \overline{S_\psi}\, dz\right].$$

(D.11)

Using (D.4), (D.9-11), and (3.9) in (D.2), we can show that

$$(\psi_u - \psi_d)_B^2\left\{-\chi_E^{-2}Ek_E\sigma_B(1-\sigma_B) + E\sigma_B\chi_E^{-1}\left[\chi_E^{-1}\sigma_B + (1-2\sigma_B)\right] - E\sigma_B(1-\sigma_B)\right\}$$
$$+(\psi_u - \psi_d)_B\chi_E^{-1}\sigma_B\int_{z_B}^{z_{B+}}\overline{S_\psi}\,dz + 2\int_{z_B}^{z_{B+}}\overline{\psi' S'_\psi}\,dz = 0 .$$

(D.12)

We require that (D.12) hold for all species, including those for which $S_\psi$ is zero. It follows that

$$\sigma_B = \frac{k_E\chi_E^2 - \chi_E + \chi_E^2}{1 + k_E\chi_E^2 - 2\chi_E + \chi_E^2} \approx \frac{k_E\chi_E^2}{1+k_E\chi_E^2},$$

(D.13a)

or, alternatively,

$$k_E = \frac{\sigma_B + \chi_E(1-2\sigma_B) - \chi_E^2(1-\sigma_B)}{\chi_E^2(1-\sigma_B)} \approx \frac{\sigma_B}{\chi_E^2(1-\sigma_B)}. \tag{D.13b}$$

Again, all reference to $\psi$ has dropped out, indicating that $k_E$ is independent of species. From (D.13b) it is apparent that $k_E$ is of order $\chi_E^{-2}$, i.e., $k_E >> 1$.

Since (D.13) must apply for all species, including those for which $S_\psi$ is *not* zero, we conclude that

$$(\psi_u - \psi_d)_B \chi_E^{-1} \sigma_B \int_{z_B}^{z_{B+}} \overline{S_\psi}\, dz + 2\int_{z_B}^{z_{B+}} \overline{\psi' S_\psi'}\, dz = 0. \tag{D.14}$$

From (D.14), we can determine the rate at which fluctuations of $S_\psi$ in the entrainment layer generate fluctuations of $\psi$ there.

Now substitute (D.8b) back into (D.3). The result is

$$2\int_{z_{S-}}^{z_S} \varepsilon_\psi \rho\, dz = \left[2(1-\sigma_S) - \chi_V(1-2\sigma_S)\right]\chi_V^{-2} V(1-\sigma_S)(\psi_u - \psi_d)_S^2. \tag{D.15}$$

Similarly, use of (D.13b) in (D.4) gives

$$2\int_{z_B}^{z_{B+}} \varepsilon_\psi \rho\, dz = \left[\sigma_B + \chi_E(1-2\sigma_B) - \chi_E^2(1-\sigma_B)\right]\chi_E^{-2} E\,\sigma_B(\psi_u - \psi_d)_B^2. \tag{D.16}$$

Using (D.15), we find that the ratio of dissipation to production, for the ventilation layer, satisfies

$$\frac{2\int_{z_{S-}}^{z_S} \varepsilon_\psi \rho\, dz}{2(F_\psi)_S(\overline{\psi}_{S-} - \overline{\psi_S})} = 1 - \left[\frac{\chi_V(1-2\sigma_S)}{2(1-\sigma_S)}\right]. \tag{D.17}$$

Similarly, using (D.16), we find that the ratio of dissipation to production, for the entrainment layer, satisfies

$$\frac{2\int_{z_B}^{z_{B+}} \varepsilon_\psi \rho\, dz}{-(F_\psi)_B \Delta\psi - E(\overline{\psi'^2})_B + 2\int_{z_B}^{z_{B+}} \overline{\psi' S_\psi'}\, dz} = 1 + \left[\frac{\chi_E(1-2\sigma_B)}{\sigma_B - \chi_E^2(1-\sigma_B)}\right]. \tag{D.18}$$

Note from (D.17) and (D.18) that, when $\chi_V$ and $\chi_E$ are small, dissipation and production must nearly balance in the ventilation and entrainment layers, respectively. Such near balances are observed, and have been predicted through LES. The entrainment and ventilation layers are typically characterized by very rapid variance production, which is nearly in balance with equally rapid variance dissipation.

APPENDIX E

# Entrainment Closure

We adopt an entrainment parameterization following the ideas of Breidenthal and Baker (1985), Siems *et al.* (1989), and Breidenthal (1989). The entrainment rate is assumed to satisfy

$$\frac{E}{\rho_B} = \sqrt{e_M} \quad \frac{b_1[1+60(\chi^* - D)]}{(1+b_2 Ri_\Delta)} \quad . \tag{E.1}$$

Here $\rho_B$ is the density at level B, $b_1$ and $b_2$ are assumed to be constants, and $\chi^*$ and $D$ are parameters (defined below) that determine the effects of evaporative cooling on the entrainment rate. The relevant Richardson number is

$$Ri_\Delta = \frac{g \Delta s_v \, \delta z_M}{c_p T_B \, e_M} \quad . \tag{E.2}$$

Here $s_v$ is the virtual dry static energy.

First consider the cloud-free case for which, as explained later, both $\chi^*$ and $D$ are zero. Then (E.1) reduces to

$$\frac{E}{\rho_B} = \sqrt{e_M} \quad \frac{b_1}{(1+b_2 Ri_\Delta)} \quad . \tag{E.3}$$

We can determine the values of $b_1$ and $b_2$ as follows. When the inversion is strong, $Ri_\Delta$ is large, and (E.3) reduces to

$$\frac{E}{\rho_B} = \sqrt{e_M} \quad \frac{b_1}{b_2 Ri_\Delta} \quad . \tag{E.4}$$

We require that this reduce to the famous "0.2" formula that has been so widely used (for a review, see Randall, 1984):

$$E \Delta s_v = 0.2 \, (F_{sv})_S \quad . \tag{E.5}$$

In order to derive (E.5) from (E.4), we assume a balance between buoyant production and dissipation of turbulence kinetic energy, i.e.

$$\tfrac{1}{2} \kappa \frac{(F_{sv})_S}{p_S} \delta p_M - \rho_M \left( \frac{e_M}{a_1} \right)^{3/2} \quad , \tag{E.6}$$

where $\kappa$ is Poisson's constant, and $a_1 \approx 0.163$ (for a discussion see Randall, 1984). From (E.4-6) we can show that $b_1 / b_2 \approx 6.10$.

A second constraint is that, for $Ri_\Delta = 0$, (E.4) should be consistent with

$$\frac{E}{\rho_B} = 0.2\, w^* , \tag{E.7}$$

where $w^*$ is the convective velocity scale of Deardorff (1970), which in the present notation is approximately given by

$$w^* = \left[ \kappa \frac{(F_{sv})_S}{(\rho p)_S} \delta p_M \right]^{1/3} . \tag{E.8}$$

The relation (E.7) was found in a large-eddy simulation by Deardorff (1974). In this no-inversion limit, (E.4) reduces to

$$\frac{E}{\rho_B} = b_1 \sqrt{e_M} . \tag{E.9}$$

We find from (E.7-9) that $b_1 \approx 0.624$. Using our earlier result, we obtain $b_2 \approx 0.102$.

Following Siems *et al.* (1989; see also Albrecht *et al.*, 1985, and Nicholls and Turton, 1986), we consider parcels consisting of a mixture of $\chi$ mass units with the properties of the air from level B+, just above the PBL top, and $(1-\chi)$ mass units with the properties of the PBL at level B, just below the PBL top. Not that if the parcels in question are descending at level B, then $\chi$ is equivalent to $\chi_E$. Let $\chi^*$ be the value of $\chi$ for which the density of the mixture is maximized. If no cloud is present, the density is simply a linear function of $\chi$, and $\chi^* = 0$. For typical stratocumulus cases, $\chi^* \leq 0.1$, while for trade cumulus cases $\chi^* \approx 0.5$.

Let

$$D \equiv -\frac{\rho(0) - \rho(\chi^*)}{\rho(0) - \rho(1)} \tag{E.10}$$

be the normalized density difference between the density of air at level B and that of the densest possible mixture. The minus sign is used to make $D$ non-negative. For the cloud-free case, $D = 0$. For typical stratocumulus cases, $D$ is slightly positive but much less than one, while for typical trade cumulus cases $D$ can be as large as three. According to Siems *et al.* (1989), $D > 1.3$ is required for cloud-top entrainment instability.

# REFERENCES


Albrecht, B. A., A. K. Betts, W. H. Schubert, and S. K. Cox, 1979: A model of the thermodynamic structure of the trade-wind boundary layer: Part I. Theoretical formulation and sensitivity tests. *J. Atmos. Sci.*, **36**, 73-89.

Albrecht, B. A., 1979: A model of the thermodynamic structure of the trade-wind boundary layer: Part II. Applications. *J. Atmos. Sci.*, **36**, 90-98.

Albrecht, B. A., R. S. Penc, and W. H. Schubert, 1985: An observational study of cloud-topped mixed layers. *J. Atmos. Sci.*, **42**, 800-822.

Arakawa, A., 1969: Parameterization of cumulus convection. *Proc. WMO/IUGG Symp. Numerical Weather Prediction*, Tokyo, 26 November - 4 December, 1968, Japan Meteor. Agency. IV, 8, 1-6.

Arakawa, A., and W. H. Schubert, 1974: The interaction of a cumulus cloud ensemble with the large-scale environment, Part I. *J. Atmos. Sci.*, **31**, 647-701.

Augstein, E., H. Schmidt, and F. Ostapoff, 1974: The vertical structure of the atmospheric planetary boundary layer in undisturbed trade winds over the Atlantic Ocean. *Bound. Layer Meteor.*,**6**, 129-150.

Augstein, E., and M. Wendel, 1980: Modelling of the time-dependent atmospheric trade-wind boundary layer with non-precipitating cumulus clouds. *Beitr. Phys. Atmos.*, **53**, 509-538.

Ball, F. K., 1960: Control of inversion height by surface heating. *Quart. J. Roy. Meteor. Soc.*, **86**, 483-494.

Betts, A. K., 1973: Non-precipitating cumulus convection and its parameterization. *Quart. J. Roy. Meteor. Soc.*, **99**, 178-196.

Benoit, R., J. Cote, and J. Mailhot, 1989: Inclusion of a TKE boundary layer parameterization in the Canadian Regional Finite-Element Model. *Mon. Wea. Rev.*, **117**, 1726-1750.

Bjerknes, J., 1938: Saturated-adiabatic ascent of air through dry-adiabatically descending environment. *Quart. J. Roy. Meteor. Soc.*, **64**, 325-330.

Breidenthal, R. E., and M. B. Baker, 1985: Convection and entrainment across stratified interfaces. *J. Geophys. Res.*, **90D**, 13055-13062.

Breidenthal, R. E., 1989: Entrainment at stratified interfaces: The effects of Schmidt, Richardson, and Reynolds numbers. Submitted to *J. Fluid Mech.*

Caughey, S. J., B. A. Crease, and W. T. Roach, 1982: A field study of nocturnal stratocumulus: II. Turbulence structure and entrainment. *Quart. J. Roy. Meteor. Soc.*, **108**, 125-144.

Chatfield, R. B., and R. A. Brost, 1987: A two-stream model of the vertical transport of trace species in the convective boundary layer. *J. Geophys. Res.*, **92**, 13263-13276.

Clarke, R. H., A. J. Dyer, R. R. Brook, D. G. Reid, and A. J. Troup, 1971:The Wangara experiment: Boundary Layer data. *Tech. Paper 19*, Div. Meteor. Phys., CSIRO, Australia.

Deardorff, J. W., 1970: Convective velocity and temperature scales for the unstable planetary boundary layer and for Rayleigh convection. *J. Atmos. Sci.*, **27**, 1211-1213.

Deardorff, J. W., 1972: Parameterization of the planetary boundary layer for use in general circulation models. *Mon. Wea. Rev.*, **100**, 93-106.

Deardorff, J.W., 1974: Three-dimensional numerical study of the height and mean structure of a heated planetary boundary layer. *Bound. Layer Meteor.*,**7**, 81-106.

Deardorff, J. W., 1980: Stratocumulus-capped mixed layers derived from a three-dimensional model. *Bound. Layer Meteor.*, **18**, 495-527.

Greenhut, G. K. and S. J. S. Khalsa, 1982: Updraft and downdraft events in the atmospheric boundary layer over the equatorial Pacific Ocean, *J. Atmos. Sci.*, **39**, 1803-1818.

Grossman, R. L., 1984: Bivariate conditional sampling of moisture flux over a tropical ocean. *J. Atmos. Sci.*, **41**, 3238-3253.

Hanson, H. P., 1981: On mixing by trade-wind cumuli. *J. Atmos. Sci.*, **38**, 1003-1014.

Khalsa, S. J. S., and G. K. Greenhut, 1985: Conditional sampling of updrafts and downdrafts in the marine atmospheric boundary layer. *J. Atmos. Sci.*, **42**, 2550-2562.

Kuo, H.-C., and W. H. Schubert, 1988: Stability of cloud-topped boundary layers. *Quart. J. Roy. Meteor. Soc.*, **114**, 887-916.

Lenschow, D. H., and P. L. Stephens, 1980: The role of thermals in the convective boundary layer. *Bound. Layer Meteor.*, **19**, 509-532.

Lenschow, D. H., and P. L. Stephens, 1982: Mean vertical velocity and turbulence intensity inside and outside thermals. *Atmos. Env.*, **16**, 761-674.

Lilly, D. K., 1968: Models of cloud-topped mixed layers under a strong inversion. *Quart. J. Roy. Meteor. Soc.*, **94**, 292-309.

Mahrt, L., and J. Paumier, 1984: Heat transport in the atmospheric boundary layer. *J. Atmos. Sci.*, **41**, 3061-3075.

Mason, P. J., 1989: Large-eddy simulation of the convective atmospheric boundary layer. *J. Atmos. Sci.*, **46**, 1492-1516.

Moeng, C.-H., 1984: A large-eddy simulation model for the study of planetary boundary-layer turbulence. *J. Atmos. Sci.*, **41**, 2052-2062.

Moeng, C.-H., 1986: Large-eddy simulation of a stratus-topped boundary layer. Part I: Structure and budgets. *J. Atmos. Sci.*, **43**, 2886-2900. .

Nicholls, S., and J. D. Turton, 1986: An observational study of the structure of stratiform cloud sheets. Part II. Entrainment. *Quart. J. Roy. Meteor. Soc.*,**112**, 461-480.

Nicholls, S., 1989: The structure of radiatively driven convection in stratocumulus. *Quart. J. Roy. Meteor. Soc.*, **115**, 487-511.

Penc, R. S., and B. A. Albrecht, 1986: Parametric representation of heat and moisture fluxes in cloud-topped mixed layers. *Bound. Layer Meteor.*, **38**, 225-248.

Randall, D. A., 1980a: Conditional instability of the first kind, upside-down. *J. Atmos. Sci.*, **37**, 125-130.

Randall, D. A.and G. J. Huffman, 1982: Entrainment and detrainment in a simple cumulus cloud model. *J. Atmos. Sci.*, **39**, 2739-2806.

Randall, D. A., 1984: Buoyant production and consumption of turbulence kinetic energy in cloud-topped mixed layers. *J. Atmos. Sci.*, **41**, 402-413.

Randall, D. A., 1987: Turbulent fluxes of liquid water and buoyancy in partly cloudy layers. *J. Atmos. Sci.*, **44**, 850-858.

Randall, D. A., P. J. Sellers, and D. A. Dazlich, 1988: Applications of a prognostic turbulence kinetic energy in a bulk boundary-layer model. *Atmospheric Science Paper No. 437*, Colorado State University, 19 pp.

Schmidt, H., and U. Schumann, 1989: Coherent structure of the convective boundary layer derived from large-eddy simulations. *J. Fluid Mech.*, **200**, 511-562.

Schubert, W. H., J. S. Wakefield, E. J. Steiner, and S. K. Cox, 1979: Marine stratocumulus convection, Part I: Governing equations and horizontally homogeneous solutions. *J. Atmos. Sci.*, **36**, 1286-1307.

Siems, S. T., C. S. Bretherton, M. B. Baker, S. Shy, and R. T. Breidenthal, 1989: Buoyancy reversal and cloudtop entrainment instability. Submitted to *Quart. J. Roy. Meteor. Soc.*

Stull, R. B., 1988: *An introduction to boundary layer meteorology*. Kluwer Academic Publ., Dordrecht, 666 pp.

Suarez, M. J., A. Arakawa, and D. A. Randall, 1983: Parameterization of the planetary boundary layer in the UCLA general circulation model: Formulation and results. *Mon. Wea. Rev.*, **111**, 2224-2243.

Wakefield, J. S., and W. H. Schubert, 1981: Mixed-layer model simulation of Eastern North Pacific stratocumulus. *Mon. Wea. Rev.*, **109**, 1952-1968.

Wang, S., and B. A. Albrecht, 1986: A stratocumulus model with an internal circulation. *J. Atmos. Sci.*, **43**, 2374-2391.

Wang, S., and B. A. Albrecht, 1990: A mean-gradient model of the dry convective boundary layer. *J. Atmos. Sci.*, **46**, 126-138.

Wilczak, J. M., and J. A. Businger, 1983: Thermally indirect motions in the convective atmospheric boundary layer. *J. Atmos. Sci.*, **40**, 343-358.

Wyngaard, J. C., and R. A. Brost, 1984: Top-down and bottom-up diffusion of a scalar in the convective boundary layer. *J. Atmos. Sci.*, **41**, 102-112.

**Table 1** Expressions for $\sigma$ and $M_C$, for the four possible combinations of unstable and stable ventilation and entrainment layers, in case both $\sigma$ and $M_C$ are independent of height.

| | *Expressions for $M_C$ and $\sigma$* | *Comments* |
|---|---|---|
| *Unstable Ventilation Layer with Stable Entrainment Layer* | $M_c = -2\hat{\Pi}_E E + 2\sqrt{\left(\hat{\Pi}_E E\right)^2 + \hat{\Pi}_E E \hat{\Pi}_V V}$<br>$\sigma = \frac{M_c}{2\hat{\Pi}_E E + M_c}$ | Can show that $0 \le \sigma \le 1$ and $M_c \ge 0$. |
| *Stable Ventilation Layer with Stable Entrainment Layer* | $M_c = 2\sqrt{\hat{\Pi}_E E \hat{\Pi}_V V}$<br>$\sigma = \frac{\hat{\Pi}_V V}{\hat{\Pi}_V V + \frac{1}{2} M_c}$ | Can show that $0 \le \sigma \le 1$ and $M_c \ge 0$. |
| *Unstable Ventilation Layer with Unstable Entrainment Layer* | $M_c = \frac{2}{3}\left(\hat{\Pi}_V V + \hat{\Pi}_E E\right) - \frac{2}{3}\sqrt{\left(\hat{\Pi}_V V - \hat{\Pi}_E E\right)^2 + \hat{\Pi}_E E \hat{\Pi}_V V}$<br>$\sigma = \frac{M_c}{2\hat{\Pi}_E E - M_c}$ | Can show that $0 \le \sigma \le 1$ and $M_c \ge 0$. As $\hat{\Pi}_E E / \hat{\Pi}_V V \to \infty$, we get $M_c \to \hat{\Pi}_V V$, and vice versa. |
| *Stable Ventilation Layer with Unstable Entrainment Layer* | $M_c = -2\hat{\Pi}_V V + 2\sqrt{\left(\hat{\Pi}_V V\right)^2 + \hat{\Pi}_E E \hat{\Pi}_V V}$<br>$\sigma = \frac{\hat{\Pi}_V V}{\hat{\Pi}_V V + \frac{1}{2} M_c}$ | Can show that $0 \le \sigma \le 1$ and $M_c \ge 0$. |

## FIGURE LEGENDS

Figure 1: Diagram summarizing the relationship of the present model to earlier models used in boundary-layer and cumulus parameterizations.

Figure 2: Diagram illustrating the assumed structure of the PBL. The interior, which is represented by two layers, is bounded above by a thin entrainment layer and below by a thin ventilation layer. Convective circulations occur, with rising branches occupying fractional area $\sigma$. The ascending and descending branches have different thermodynamic soundings and, therefore, different cloud base levels.

Figure 3: Sketch illustrating the step-function pdf for $\chi$ in the ventilation layer.

Figure 4: Plots of $\sigma$ and $M_C$ as functions of $\eta$. "UVSE" denotes unstable ventilation layer with stable entrainment layer; "UVUE" denotes unstable ventilation layer with unstable entrainment layer; "SVSE" denotes unstable ventilation layer with unstable entrainment layer; and finally "SVUE" denotes unstable ventilation layer with unstable entrainment layer.

Figure 5: A plot of $s_v(\chi) - \overline{s_{vB}}$ as a function of $\chi$, for a case in which CTEI is predicted by the criterion of Randall (1980), with $\Delta s_v - (\Delta s_v)_{crit}$ = - 5.4 kJ kg$^{-1}$, but not by the criterion of Siems *et al.* (1989), with $D$ = 0.32 and $\chi^*$ = 0.12. We have assumed $p_B$ = 950 mb, $z_B$ = 597 m, $\bar{h}_B$ = 315.0 kJ kg$^{-1}$, $\bar{r}_B$ = 9.53 g kg$^{-1}$, $\bar{h}_{B+}$ = 299.3 kJ kg$^{-1}$, and $\bar{r}_{B+}$ = 1.0 g kg$^{-1}$. The liquid water mixing ratio corresponding to the mean conditions at level B is 0.33 g kg$^{-1}$.

Figure 6: The solid line shows $\sigma_B$ as a function of $E / M_{cB}$ for the data of Fig. 5. For comparison, the dashed line shows the predictions of (3.31) (for the stable cloud-free case) and the dotted line shows the predictions of (3.32) (for the unstable cloud-free case).

Figure 7: As in Fig. 5, but for a case in which cloud-top entrainment instability is predicted to occur. CTEI is predicted, with $\Delta s_v - (\Delta s_v)_{crit}$ = - 7.3 kJ kg$^{-1}$, $D$ = 1.96 and $\chi^*$ = 0.49. We have assumed $p_B$ = 850 mb, $z_B$ = 1533 m, $\bar{h}_B$ = 333.2 kJ kg$^{-1}$, $\bar{r}_B$ = 14.75 g kg$^{-1}$, $\bar{h}_{B+}$ = 308.7 kJ kg$^{-1}$, and $\bar{r}_{B+}$ = 1.0 g kg$^{-1}$. The liquid water mixing ratio corresponding to the mean conditions at level B is 2.84 g kg$^{-1}$.

Figure 8: As in Fig. 6, but for the case illustrated in Fig. 7.

Figure 9: Three profiles of $h(\chi)$, for different choices of $\delta h_R(\chi)$ . The dotted curve shows the case for which $\delta h_R(\chi)$ is zero. The dashed curve illustrates the situation for which $\delta h_R(\chi)$ is negative and independent of $\chi$. The dotted curve illustrates a case in which $\delta h_R(\chi)$ is more strongly negative for smaller values of $\chi$.

Figure C1: Two values of $\chi$ for which the virtual dry static energies of the mixed parcels are the same. The value of $\chi$ corresponding to saturation is called $\chi_1$, and the value of $\chi$ corresponding to subsaturation is called $\chi_2$.

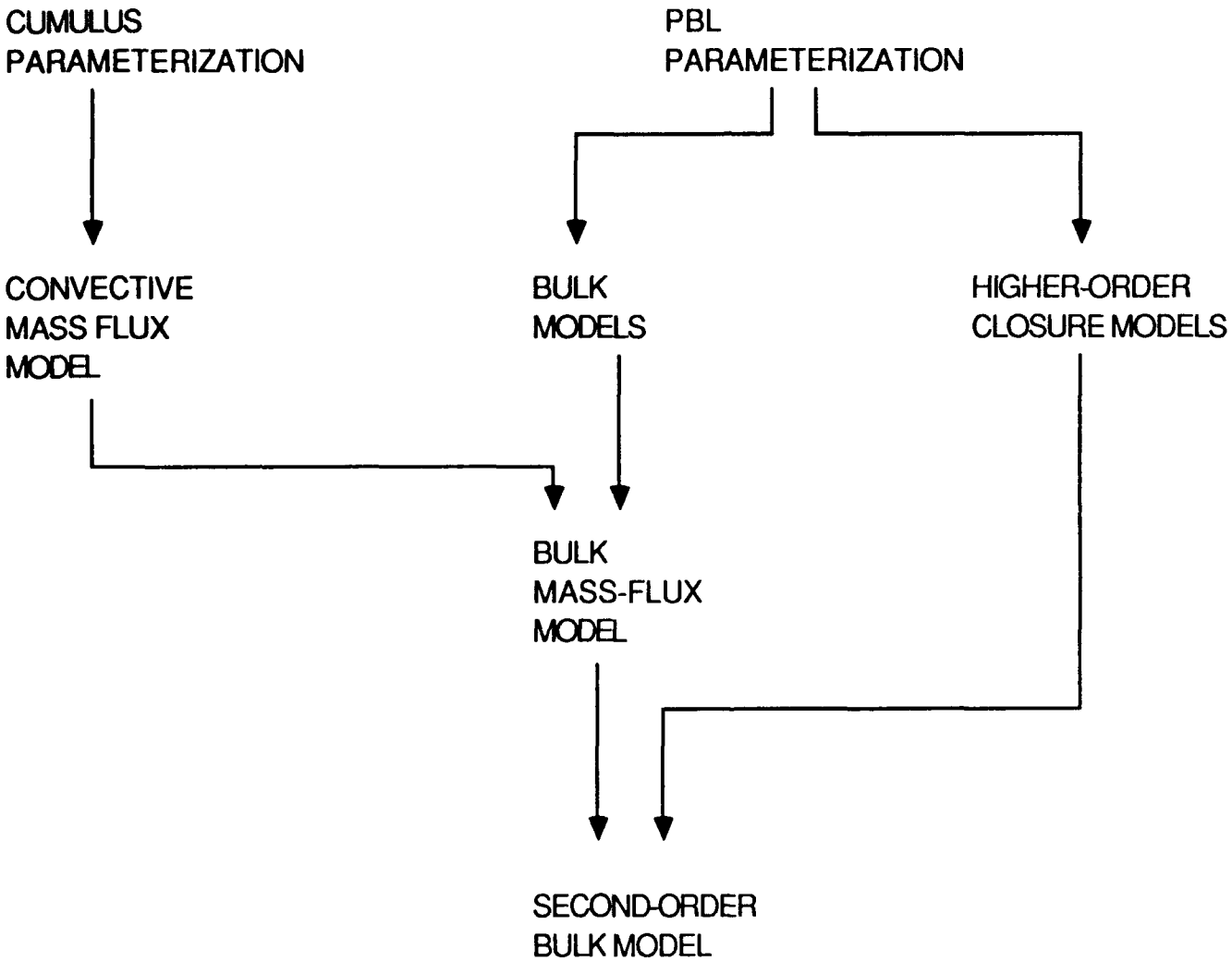
CUMULUS
PARAMETERIZATION
PBL
PARAMETERIZATION
CONVECTIVE
MASS FLUX
MODEL
BULK
MODELS
HIGHER-ORDER
CLOSURE MODELS
BULK
MASS-FLUX
MODEL
SECOND-ORDER
BULK MODEL

Fig. 1

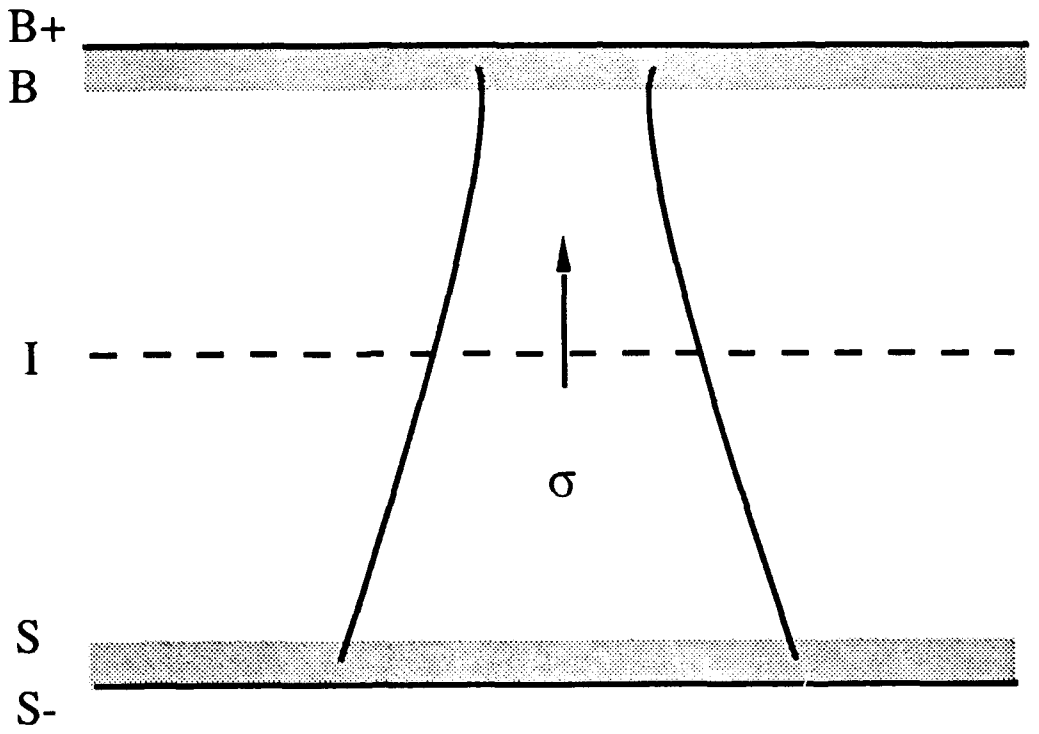


Fig. 2

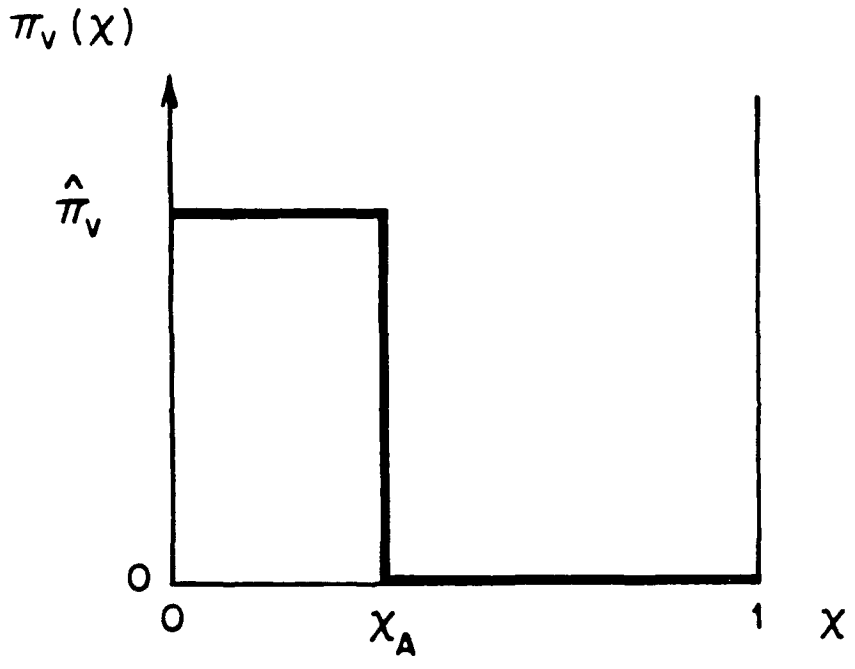


Fig. 3

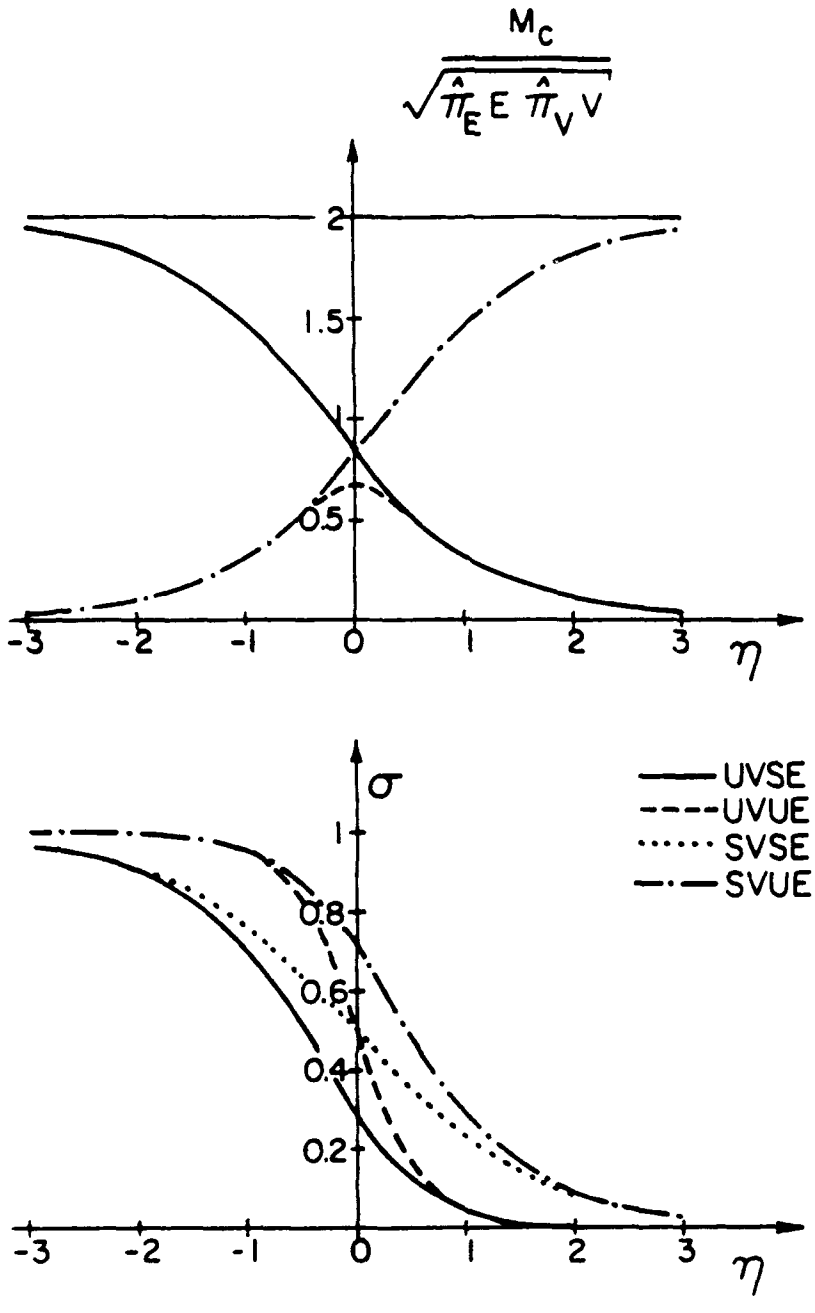
$\frac{M_C}{\sqrt{\hat{\pi}_E E \, \hat{\pi}_V V}}$
2
1.5
1
0.5
-3
-2
-1
0
1
2
3
$\eta$
$\sigma$
UVSE
UVUE
SVSE
SVUE
1
0.8
0.6
0.4
0.2
-3
-2
-1
0
1
2
3
$\eta$

Fig. 4

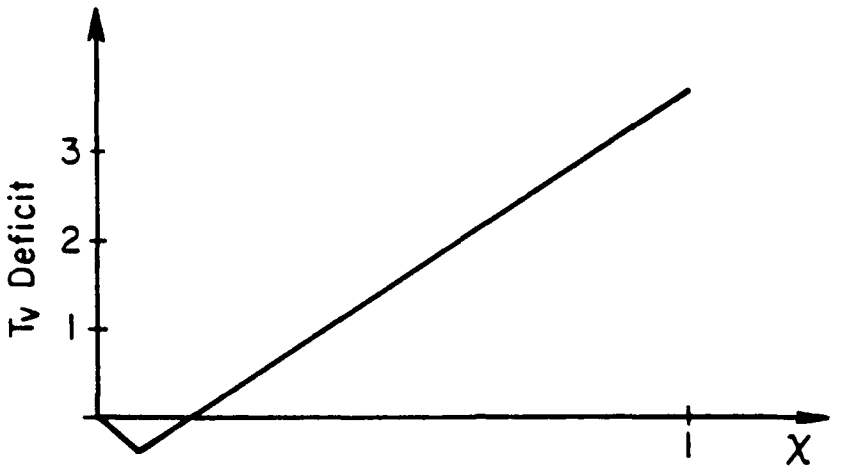


Fig. 5

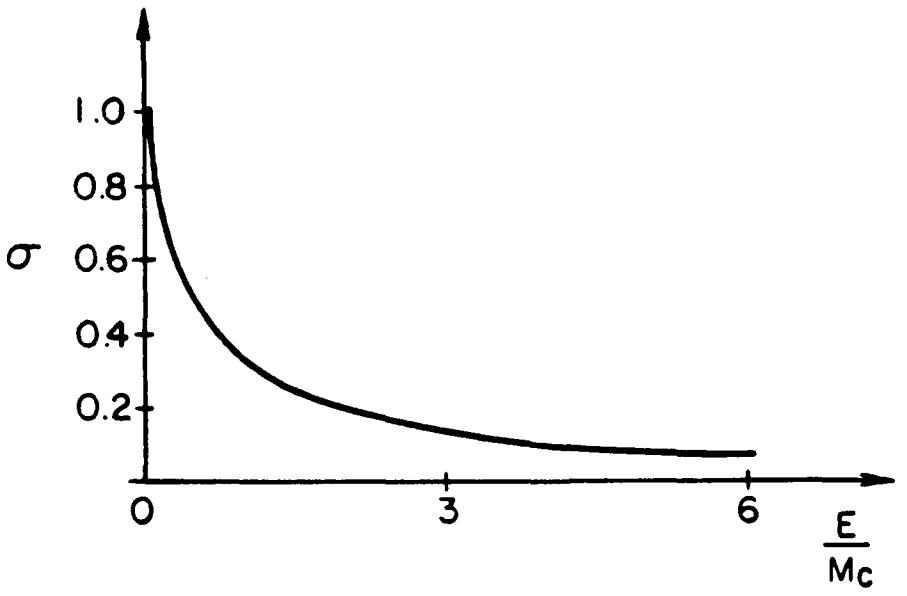


Fig. 6

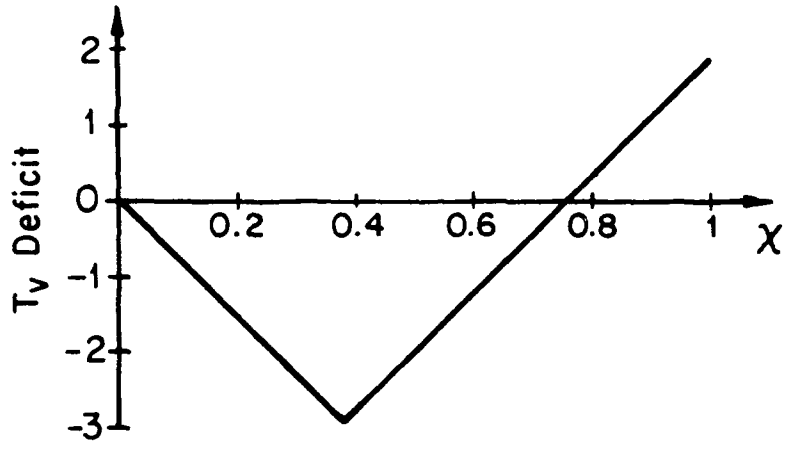


Fig. 7

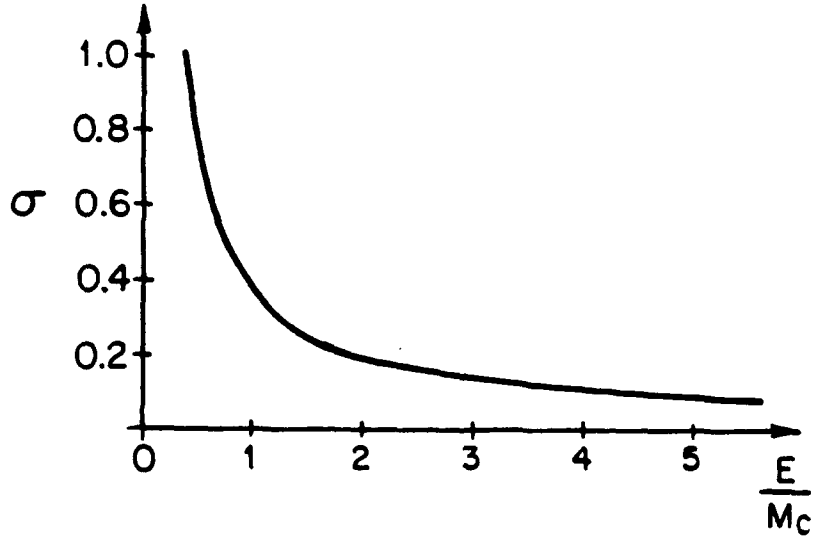


Fig. 8

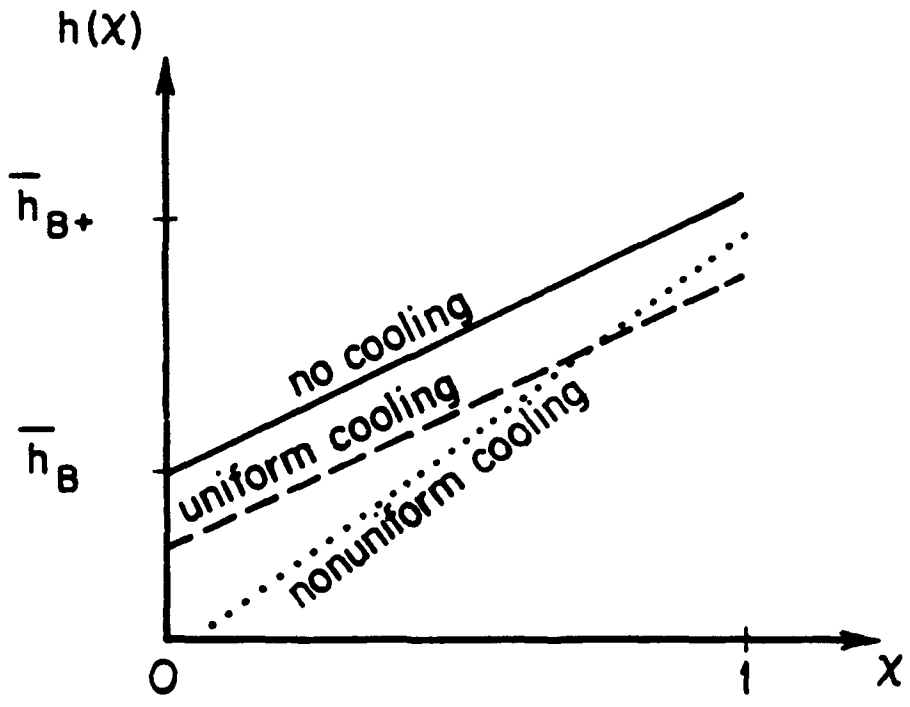
h(X)
$\overline{h}_{B+}$
$\overline{h}_{B}$
no cooling
uniform cooling
nonuniform cooling
0
1
X

Fig. 9

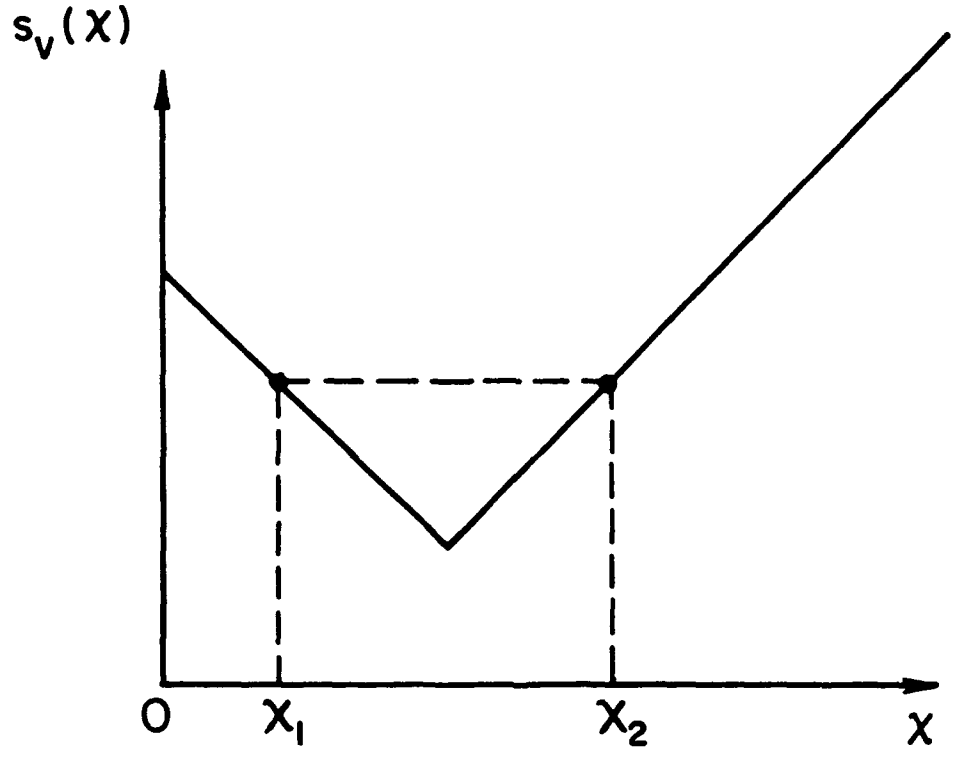


Fig. C1